NAVAL POSTGRADUATE SCHOOL
Monterey, California

THESIS

ARIES NAVIGATION SYSTEM ACCURACY AND TRACK FOLLOWING

by

Thanh V. Nguyen

March 2002

Thesis Advisor: Anthony J. Healey

Approved for public release; distribution is unlimited

THIS PAGE INTENTIONALLY LEFT BLANK

REPORT DOCUMENTATION PAGE			Form Approved OMB No. 0704-0188
Public reporting burden for this collection of information is estimated to average 1 hour per response, including the time for reviewing instruction, searching existing data sources, gathering and maintaining the data needed, and completing and reviewing the collection of information. Send comments regarding this burden estimate or any other aspect of this collection of information, including suggestions for reducing this burden, to Washington headquarters Services, Directorate for Information Operations and Reports, 1215 Jefferson Davis Highway, Suite 1204, Arlington, VA 22202-4302, and to the Office of Management and Budget, Paperwork Reduction Project (0704-0188) Washington DC 20503.			
1. AGENCY USE ONLY *(Leave blank)*	**2. REPORT DATE** March 2002	**3. REPORT TYPE AND DATES COVERED** Master's Thesis	
4. TITLE AND SUBTITLE: ARIES Navigation System Accuracy and Track Following			**5. FUNDING NUMBERS**
6. AUTHOR(S): Thanh V. Nguyen			
7. PERFORMING ORGANIZATION NAME(S) AND ADDRESS(ES) Naval Postgraduate School Monterey, CA 93943-5000			**8. PERFORMING ORGANIZATION REPORT NUMBER**
9. SPONSORING /MONITORING AGENCY NAME(S) AND ADDRESS(ES) N/A			**10. SPONSORING/MONITORING AGENCY REPORT NUMBER**
11. SUPPLEMENTARY NOTES The views expressed in this thesis are those of the author and do not reflect the official policy or position of the Department of Defense or the U.S. Government.			
12a. DISTRIBUTION / AVAILABILITY STATEMENT Approved for public release; distribution is unlimited			**12b. DISTRIBUTION CODE**

13. ABSTRACT ***(maximum 200 words)***

One of the greatest challenges associated with the Autonomous Underwater Vehicle (AUV) is reliability, accuracy, and the high precision navigation system for its submerged operations. Data collected for later analysis can be meaningful if, and only if, the precise location of the vehicle is known at the time the information is recorded. A reliable AUV must be able to determine its global position in the absence of external transmitting devices. Dead reckoning is unreliable because of current conditions and random errors in the velocity measurement that can be integrated and propagated in position calculations for long distance submerged travel. The alternative is the optimal integration of all available organic vehicle sensors to determine vehicle position. This requires the Kalman filtering method which merges all available vehicle sensors to estimate position. The AUV ARIES was operated in the Azores from August 10-12, 2001. All information were recorded and transferred into several files for all the mission runs during the exercise. This thesis investigated the accuracy of the Kalman filter navigation system during those runs. The thesis also examines the actual vehicle tracks during the experiment with both the design tracks and the model prediction tracks built using a simulation of the vehicle track following behavior.

14. SUBJECT TERMS Navigation, Track Following			**15. NUMBER OF PAGES** 97
			16. PRICE CODE
17. SECURITY CLASSIFICATION OF REPORT Unclassified	**18. SECURITY CLASSIFICATION OF THIS PAGE** Unclassified	**19. SECURITY CLASSIFICATION OF ABSTRACT** Unclassified	**20. LIMITATION OF ABSTRACT** UL

NSN 7540-01-280-5500 Standard Form 298 (Rev. 2-89)
Prescribed by ANSI Std. 239-18

THIS PAGE INTENTIONALLY LEFT BLANK

Approved for public release; distribution is unlimited

ARIES NAVIGATION SYSTEM ACCURACY AND TRACK FOLLOWING

Thanh V. Nguyen
Lieutenant Commander, United States Navy
B.S., University of Memphis, 1989

Submitted in partial fulfillment of the
requirements for the degree of

MASTER OF SCIENCE IN MECHANICAL ENGINEERING

from the

NAVAL POSTGRADUATE SCHOOL
March 2002

Author: Thanh V. Nguyen

Approved by: Anthony J. Healey
Thesis Advisor

Terry R. McNelley
Chairman, Department of Mechanical Engineering

THIS PAGE INTENTIONALLY LEFT BLANK

ABSTRACT

One of the greatest challenges associated with the Autonomous Underwater Vehicle (AUV) is reliability, accuracy, and the high precision navigation system for its submerged operations. Data collected for later analysis can be meaningful if, and only if, the precise location of the vehicle is known at the time the information is recorded. A reliable AUV must be able to determine its global position in the absence of external transmitting devices. Dead reckoning is unreliable because of current conditions and random errors in the velocity measurement that can be integrated and propagated in position calculations for long distance submerged travel. The alternative is the optimal integration of all available organic vehicle sensors to determine vehicle position. This requires the Kalman filtering method which merges all available vehicle sensors to estimate position. The AUV ARIES was operated in the Azores from August 10-12, 2001. All information were recorded and transferred into several files for all the mission runs during the exercise. This thesis investigated the accuracy of the Kalman filter navigation system during those runs. The thesis also examines the actual vehicle tracks during the experiment with both the design tracks and the model prediction tracks built using a simulation of the vehicle track following behavior.

THIS PAGE INTENTIONALLY LEFT BLANK

TABLE OF CONTENTS

THIS PAGE INTENTIONALLY LEFT BLANK

LIST OF FIGURES

LIST OF TABLES

THIS PAGE INTENTIONALLY LEFT BLANK

ACKNOWLEDGMENTS

This thesis research would not have possible without the guidance, patience, support, encouragement, and understanding of my thesis advisor, Professor Anthony J. Healey. I would like to express my sincere gratitude to him. His thorough knowledge in the area of Autonomous Underwater Vehicles, marine vehicle dynamics, and MATLAB code provided one of the best possible research opportunities for my work. His compassion as a professor, and his enthusiasm for the development of a highly accurate and reliable Autonomous Underwater Vehicle for the Navy are second to none. His desire for students to succeed, graduate, and continue with their careers in the Navy was clear when he accepted me as one of his thesis students very late in the graduate program. For each of these things, I will be forever grateful.

Finally, I would like to thank my wife, Amy, and my children Jacob, Kaley, Josie, and Madison for their patience and understanding when I could not devote all the attention to them that they deserve.

THIS PAGE INTENTIONALLY LEFT BLANK

I. INTRODUCTION

A. BACKGROUND

Throughout naval history, especially in the last fifteen years, when compared with modern aircraft carriers, combatant ships, and submarines, mine warfare ships have been a somewhat less glamorous aspect of the profession. When a mine struck the USS Samuel B. Roberts in 1988 and during the Persian Gulf War, mines made naval warships vulnerable. Mines are inexpensive to produce and they do not require a lot of sophisticated technology. Mine warfare is effective and represents the single largest threat to naval forces operating in shallow water regions. Since the end of World War II, more than 80 percent of the U.S. Navy ships damaged by enemy action were the victims of mines. Naval leadership has overlooked the threat of mines. As a result, our adversaries have been able to use mine warfare to their advantage. When the USS Princeton and USS Tripoli struck a World War II mine during the Persian Gulf War, it became clear that the mine problem reaches farther than littoral regions. Mines disrupt our ability to project power at sea and our ability to conduct amphibious landings on enemy shorelines [Ref. 3].

Today's naval forces have very limited capability to counter the mine threat. The U.S. mine countermeasures force consists of mine warfare ships, Explosive Ordnance Disposal units, and helicopters equipped with the latest airborne mine detection and neutralization systems. These solutions are the first step toward achieving a robust mine warfare capability in the naval forces. To graduate from a limited detection and avoidance capability to a level that can perform the full spectrum of covert functions, the Navy will need a network of Autonomous Underwater Vehicles (AUV) [Ref. 2]. These will have sensors and the capability to conduct covert mine warfare operations after being launched from their "mother" platforms. This thesis investigated the navigation system accuracy of the AUV ARIES and examines the actual vehicle tracks during the experiment with both the design tracks and the model prediction tracks built using a simulation of the vehicle track following behavior.

B. UNDERWATER VEHICLE NAVIGATION CONCERNS

The primary concern for AUV systems is the reliability, accuracy, and high precision navigation system for its submerged operations [Ref. 1]. Data collected for later analysis can be meaningful if, and only if, the precise position of the vehicle is known at the time the information is recorded. A map of the ocean floor infested with mines is very crucial to the decision making in the conduct of our amphibious operations. This map is useless if the AUV position or the reference point is unknown. Dead reckoning is the most basic navigation method for underwater vehicles with no inertial system. This method measures the distance traveled by multiplying the measured velocity by a fixed interval of time to obtain distance traveled from a known reference position. Together with a heading sensor, vehicle track can be obtained. For long distance, this method is unreliable because of current conditions and random error in the velocity and heading measurements are integrated and propagated in position calculations between DGPS updates. For the past decade, the Naval Postgraduate School AUV used a precision gyroscope and the Kalman filter [Ref. 10]. The Kalman filter integrates the data from different sensors such as: velocity, and heading with the time of GPS update. The complexity of the Kalman filter resides in many different input states. With the information from all these states, the Kalman filter optimally integrates data and recursively processes the measurements to provide the best estimate of vehicle position. Although several sensors are inputs to the vehicle control system, the most important sensors in this integration process are the velocity sensor and the sensor that provides the heading reference. References 6, and 10 provide details on Kalman filtering and its use in small AUV navigation system.

C. SCOPE OF THESIS

The main focus of this thesis is to analyze the navigation error resulting from the 1200kHz RD instruments navigator Doppler Velocity Log that contains a TCM 2 magnetic compass. The thesis will also evaluate the track error percentage as a function of distance the autonomous vehicle travels while submerged.

Chapter II provides an overview of the vehicle. A brief physical description includes dimensions, construction materials, and major hardware components. Operational capability is also explained. This chapter puts forth information on the

ARIES AUV, the vehicle being developed, tested, and upgraded by the NPS AUV research group. Vehicle underwater flight operational parameters and its mission are entailed.

Chapter III explains the when and where the experimental testing was conducted on the ARIES AUV.

Chapter IV explains the approach and methodologies in which data from the Azores were analyzed.

Chapter V documents the results of navigational error one can expect when the AUV travels submerged. Prediction of error between vehicle tracks versus programmed tracks with and without current conditions is also included. This chapter also summarizes the conclusions of this thesis on ARIES AUV detailed in Chapters IV and makes recommendations regarding on future testing associated with this topic on AUV.

THIS PAGE INTENTIONALLY LEFT BLANK

II. VEHICLE OVERVIEW

A. NPS AUTONOMOUS UNDERWATER VEHICLE

Faculty and students from the Naval Postgraduate School's Graduate School of Engineering and Applied Science comprise the NPS AUV Research Group that was started in 1987 to advance the development of the PHOENIX and ARIES autonomous underwater vehicles and their control and navigation performance [Ref. 3]. The current testing platform for the research group is the ARIES AUV. This vehicle is an updated version of the "PHOENIX" vehicle. ARIES is a shallow water communications server vehicle with a global positioning system (GPS) and a doppler aided inertial measurement unit (IMU). Navigational errors are corrected by the DGPS when the underwater vehicle surfaces. This vehicle has supported research on various control system architectures, as well as equipment reliability, navigation accuracy, and communications performance. The vehicle is shown in a DGPS pop-up maneuver in the Azores in Figure 1.

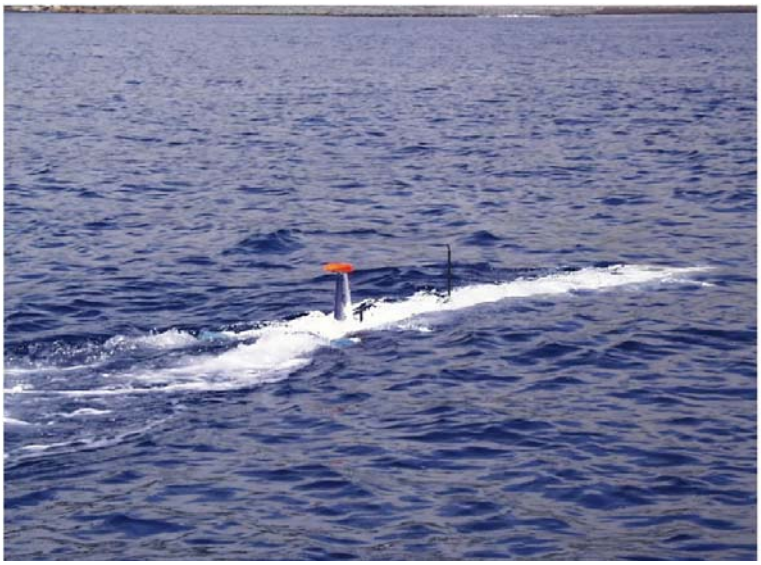

Figure 1. The NPS AUV in a GPS Pop-Up Maneuver in the Azores (August 2001).

The Aries hull was outfitted in the fall of 1999 and has recently become fully operational in the spring of 2000. This vehicle has been designed to test and demonstrate its ability to perform for a network server platform, ocean survey, targets reacquisition,

and navigational accuracy during AUV Fest in Gulfport, Mississippi in 1999. Figure 2 shows the command and control system during Azores operation on August 2001.

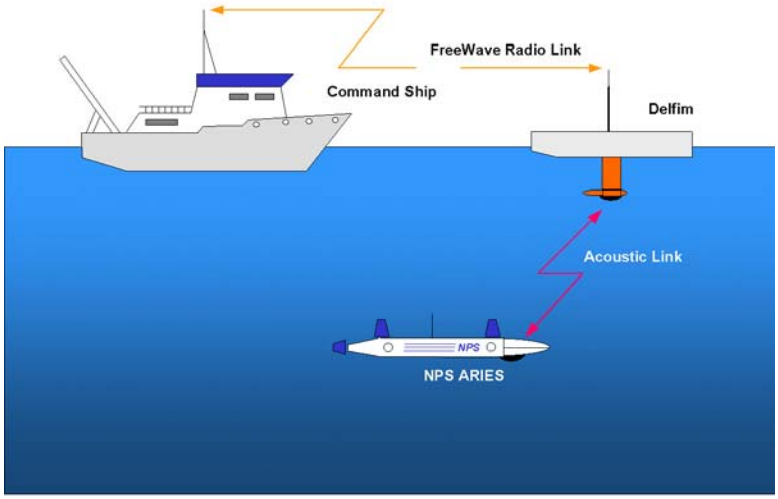

Figure 2. Aries Command and Control System for the August, 2001 Exercise.

B. VEHICLE DESCRIPTION

The major hardware components of the ARIES are shown in Figure 3 and are described below. The vehicle weighs 225 kg and measures 0.4 m wide, 0.25 m high, and approximately 3m long. The hull is constructed of 0.25 inch thick 6061 aluminum. It forms the main pressure hull that houses all electronic components, sensors, computers, and six 12 volts rechargeable lead acid batteries [Ref. 1]. It is designed to maintain a top speed of 3 - 4 knots for 3 hours and can operate safely at a depth of 30 meters. Main propulsion is achieved using twin 0.5 HP electric drive thrusters located at the stern of the vehicle. During normal flight operation, depth dive and heading are controlled by a combination of upper bow, stern rudders, bow planes, and stern planes.

Various onboard sensors serve to either collect data or provide necessary information to the AUV control systems. These sensors are:

- Depth cell and Systron Donner 3 (IMU) MotionPak
- Tri-tech ST725 (scanning sonar for obstacle avoidance and target acquisition/reacquisition)
- 1200 kHz RD instruments navigator Doppler Velocity Log that contains a TCM 2 magnetic compass (navigational sensors)

- Kearfort KG 2000 Gyro system
- Honeywell HG 3000 magnetorestructive compass

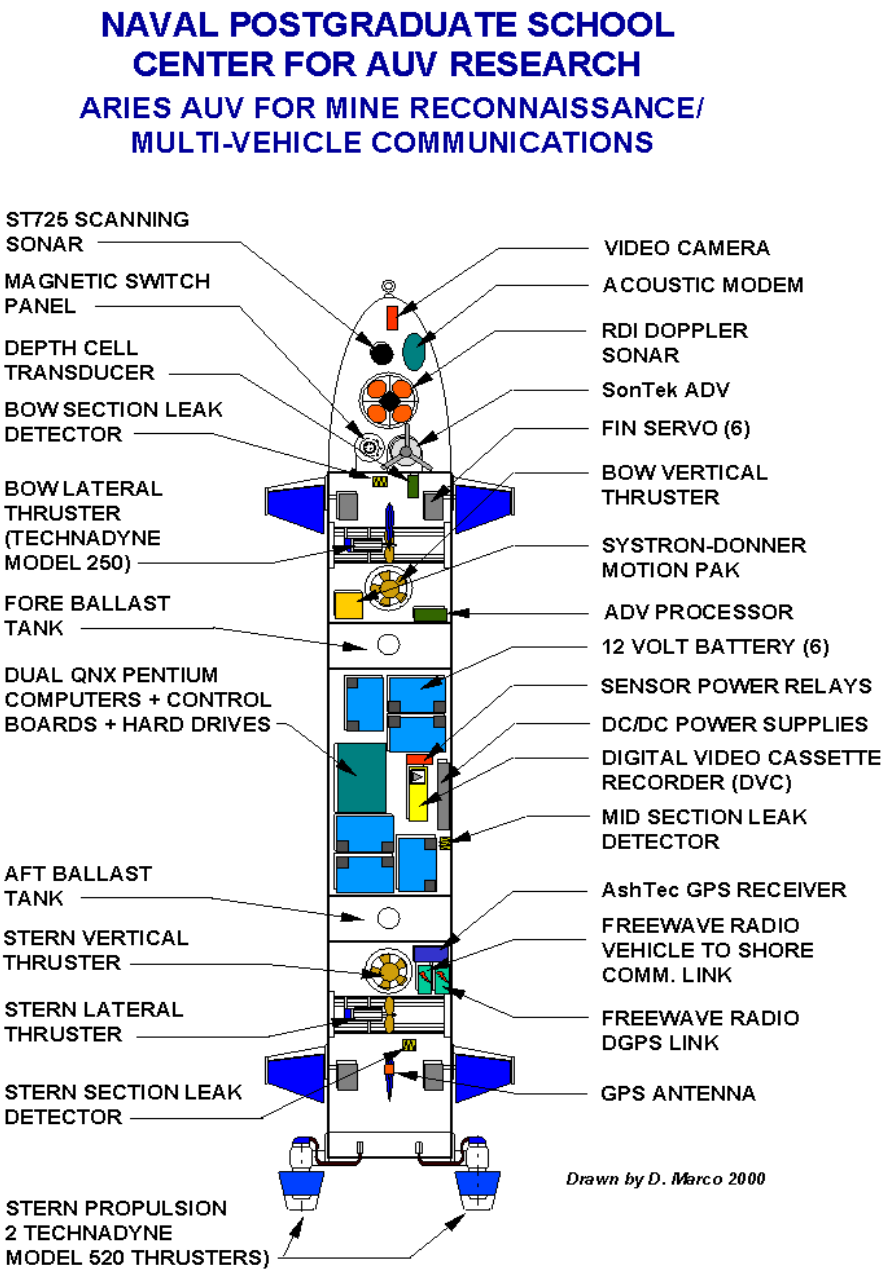

Figure 3. Naval Postgraduate School AUV Aries.

THIS PAGE INTENTIONALLY LEFT BLANK

III. EXPERIMENTAL TESTING

A. GENERAL

Faculty members from the Graduate School of Engineering and Applied Science, the Instituto of Superior Technico (IST), and the University of Azores have had a long standing agreement for the exchange of technology concerning AUV. The three schools have shared effort on the evaluation, research, system methodologies, and mission specifications of the AUV. An experimental mission was conducted around the island of Faial in the Azores during August 2001 comparing ARIES and DELFIM. The experiments facilitated analysis of the underwater navigation system, their ability to follow the preprogrammed tracks, and acoustic communication links for command and data transfer between the two vehicles. Professor Anthony Healey, Dr. Dave Marco, and Mr. Robert Dayak from NPS flew to the Azores in early August 2001 with the AUV Aries. The vehicle has a video capability using a deep sea power light multi seacam camera, and an acoustic modem for underwater communications using a new modem under development at Florida Atlantic University. Diving support and surface ship support were provided by the University of Azores and Azores Department of Fisheries. The second autonomous underwater vehicle named DELFIM was provided by the University of Lisbon. For the experimental mission, a pair of acoustic modems was installed on the ARIES and DELFIM. Two laptop computers were used on the vessel, Arquipelago, which served as the base station for this exercise. Communications were directed from the surface ship Arquipelago to the surface AUV DELFIM which, in turn, transferred data to the submerged AUV ARIES through an acoustic modem mounted below the AUV DELFIM. Figure 4 shows the map of the Azores operational area. ARIES being loaded onto the vessel Arquipelago is showed in Figure 5, and ARIES at one meter depth operated by the research vessel Arquipelago is showed in Figure 6. ARIES and DELFIM at the operational area are seen from the vessel Arquipelago in Figure 7.

Figure 4. Map of the Island of Faial, Azores-Operational Area Northeast of Horta.

Figure 5. ARIES being Loaded onto the Research Vessel Arquipelago (August 09, 2001).

Figure 6. Arquipelago and ARIES - at 1 Meter Depth on August 12, 2001.

Figure 7. ARIES and DELFIM at Operational Area.

B. ACTIVITIES CONDUCTED

Day-to-day activities are listed in Table 1 below.

Date	Activities
Monday, August 6	Arrived, unpack Aries
Tuesday, August 7	Partial re-assembly of Aries
Wednesday, August 8	System connections and testing
Thursday, August 9	Acoustic modem software integration and testing
Friday, August 10	Deployment of Aries to Arquipilago Modem test and evaluation in harbor ballast tests in harbor. Transit to site, mission 0
Saturday, August 11	Transit to site navigation tests of Aries at site, development of new deviation table; Mission 1, 2, 3 - Navigation
Sunday, August 12	Missions 4,5,6. Missions 7,8,9
Monday, August 13	Off-load Aries
Tuesday, August 14	Pack up Aries for transportation
Wednesday, August 15	Pack up Aries for transportation

Table 1. List of Daily Activity.

Files obtained for navigational accuracy studies are given in Table 2 below.

Data File	Comments
Mission 0; d081001_01.d	In harbor Communications Tests
Mission 1; d081101_01.d	Navigation test
Mission 2; d081101_02.d	Navigation test
Mission 3; d081101_03.d	Navigation test
Mission 4; d081201_01.d	Video acquisition tests
Mission 5; d081201_02.d	Video acquisition tests
Mission 6; d081201_03.d	Video acquisition tests
Mission 7; d081201_04.d	Acoustic communications tests
Mission 8; d081201_05.d	Acoustic communications tests
Mission 9; d081201_06.d	Acoustic communications tests

Table 2. List of Navigation Files and Tracks.

C. DATA COLLECTION

After initializing the Aries and Delfim computers and allowing the DG to spin up and stabilize, the research vessel Arquipelago launched the AUVs into the operational area. The AUV research group conducted several tests with the ARIES and DELFIN to

establish communication between all three vehicles. Communications between all three vehicles were tested and the results were satisfied. Data was then collected and stored at a sampling rate of 8 hertz for all missions. These data are useful for analysis of navigation error and comparison of actual vehicle tracks with preprogrammed tracks as described in Chapters IV and V.

THIS PAGE INTENTIONALLY LEFT BLANK

IV. METHODOLOGIES OF DATA ANALYSIS

A. NAVIGATION ERROR

The AUV ARIES uses an inertial navigation system, Doppler, DGPS navigational suite and an extended Kalman filter [Ref. 10]. This navigation system may be tuned for optimal performance given a set of data. The Kalman filter integrates data from different sensors such as velocity, heading, and speed over ground, etc. The complexity of the Kalman filter resides in an 8-state non-linear model of vehicle motion. The Kalman filter optimally integrates data and recursively processes the measurements to improve system performance. The most important sensors are those for speed over ground and heading reference. The heading reference is derived from both the compass, located in the RDI navigator, and the Systron Donner (IMU), which provides yaw rate. The combination fusion of the yaw rate and the compass data leads to an identification of the yaw rate bias, which is assumed to be a constant value. The sensors provide input to the vehicle control system. When the vehicle is submerged, the heading bias is unobservable and will continue to grow until a new update is obtained [Ref. 5]. When the vehicle surfaces for a short time of approximately ten seconds, the Kalman filter and new GPS update serve to correct the estimation of all states. This position error is corrected by allowing the filter to re-estimate biases and, thereby, improve accuracy. The AUV Aries was operated in the Azores from August 10-12, 2001 in a series of runs that included a dive-surface-dive-surface sequence. Data was retrieved from the file and analyzed for position error when the vehicle was submerged. While the AUV Aries was submerged, it was unable to receive GPS signals from all the available orbiting satellites. Therefore, it utilized its own Kalman filter navigation system to determine the vehicle location at all time [Ref. 6]. When the AUV Aries surfaced after a dive, it received GPS signals from all the available satellites. The Kalman filter re-estimated biases, corrected position estimates and continued to improve accuracy. For the mission run on August 11, 2001, data from six dive-surface operations were extracted from the vehicle's internal file. Figures 8 through 13 compare vehicle locations obtained from GPS with locations calculated from the vehicle's internal navigation system. The differences in location are shown in meters in

the Y-axis ant the time in second in the X-axis. Total submerged time for the AUV Aries varied between 87 to 546 seconds.

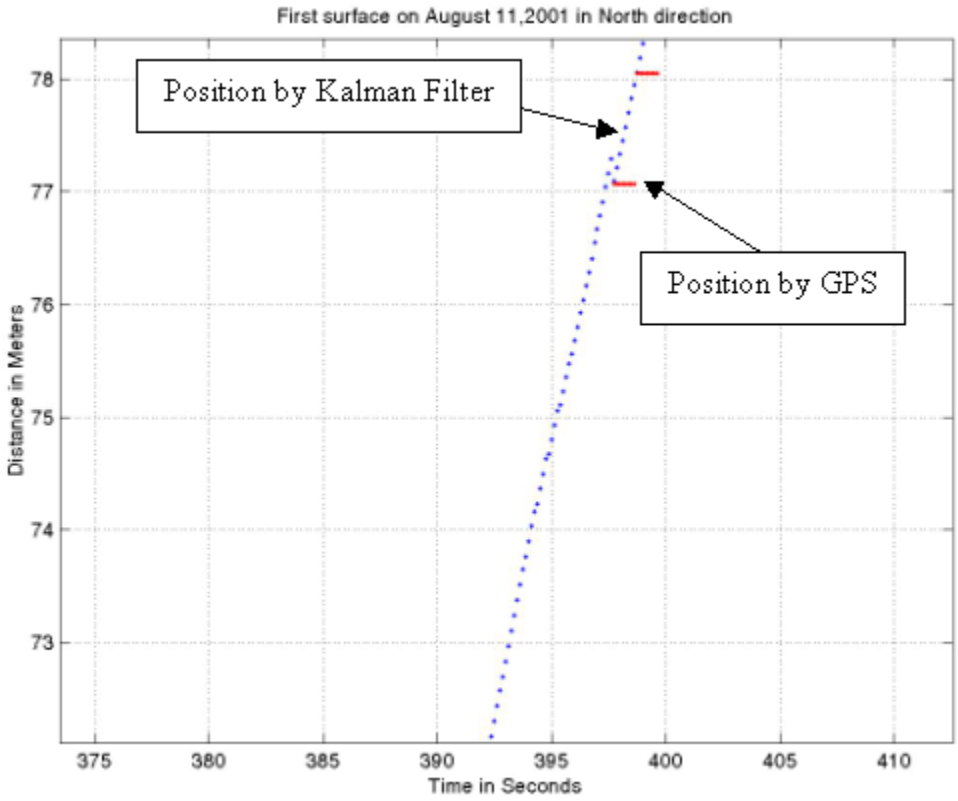

(a)

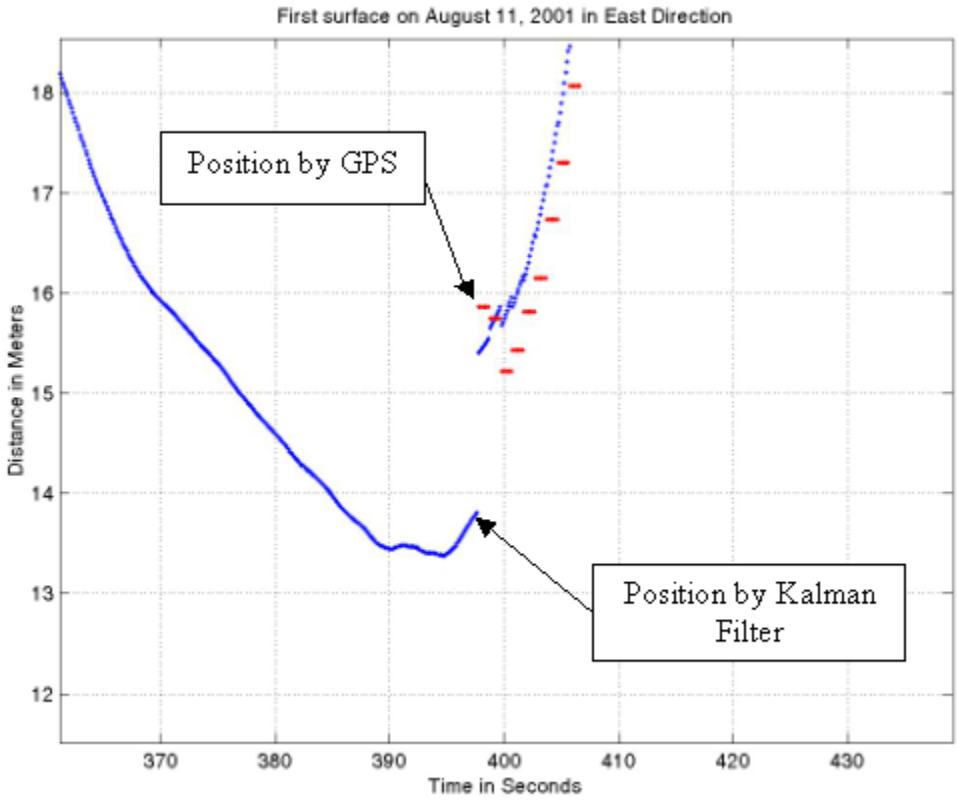

(b)

Figure 8. (a) Differences between GPS and Internal Navigation in the North Direction for the 1st Surface on August 11, 2001 (b) Differences between GPS and Internal Navigation in the East/West Direction for the 1st Surface on August 11, 2001.

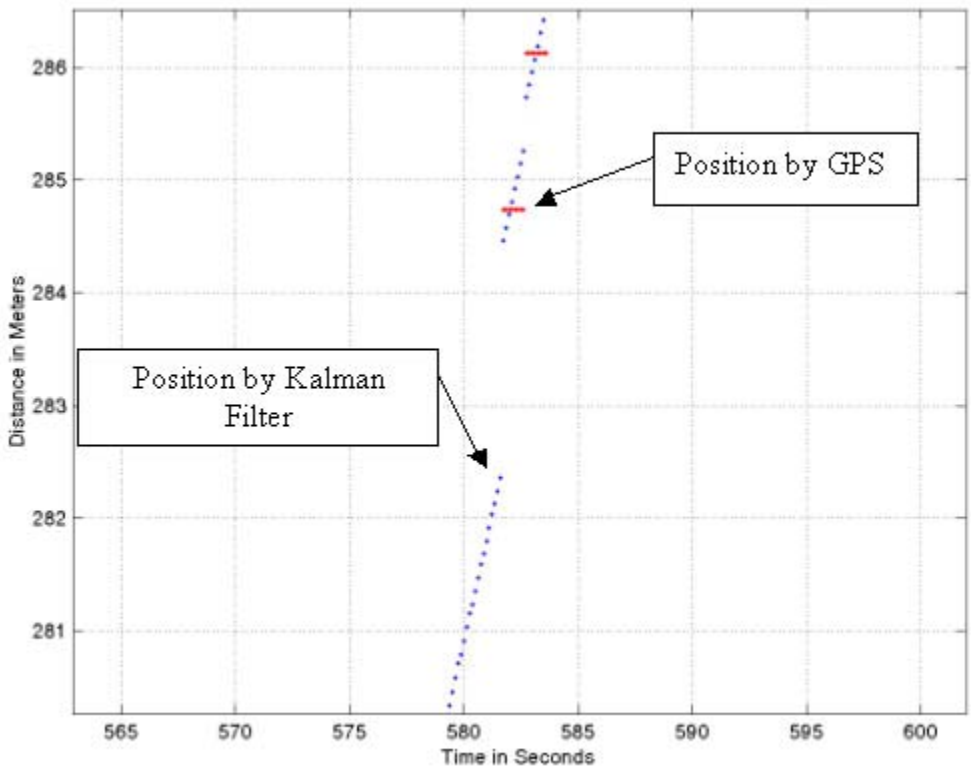
Position by GPS
Position by Kalman Filter
Distance in Meters
Time in Seconds
286
285
284
283
282
281
565
570
575
580
585
590
595
600

(a)

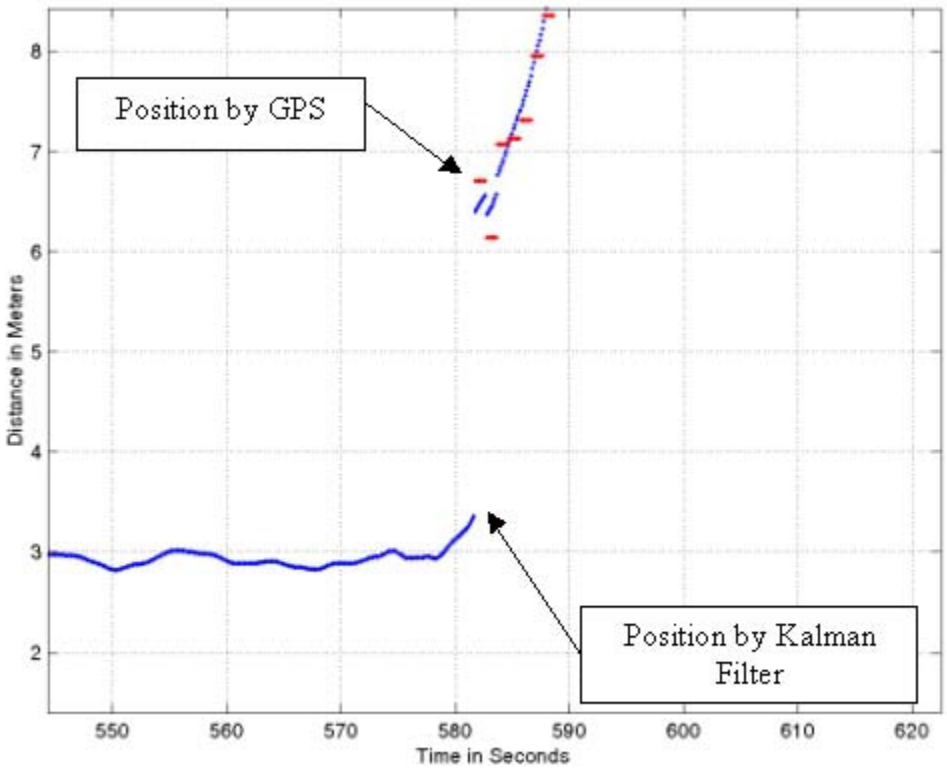

(b)

Figure 9. (a) Differences between GPS and Internal Navigation in the North Direction for the 2nd Surface on August 11, 2001 (b) Differences between GPS and Internal Navigation in the East/West Direction for the 2nd Surface on August 11, 2001.

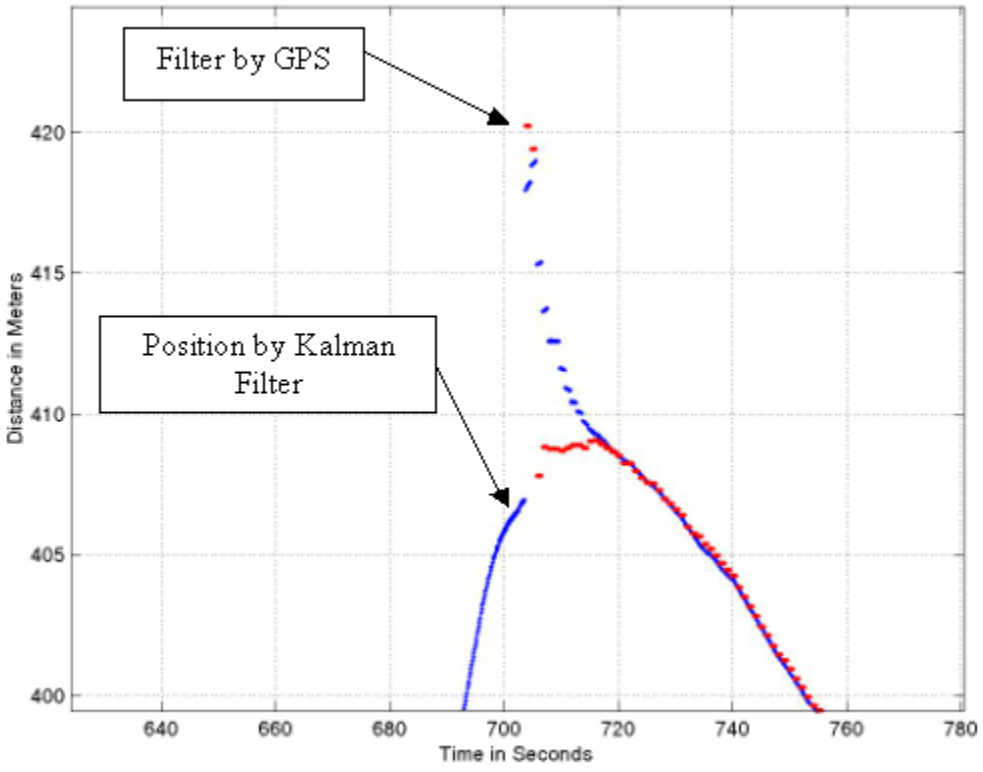
Filter by GPS
Position by Kalman Filter
Distance in Meters
Time in Seconds
420
415
410
405
400
640
660
680
700
720
740
760
780

(a)

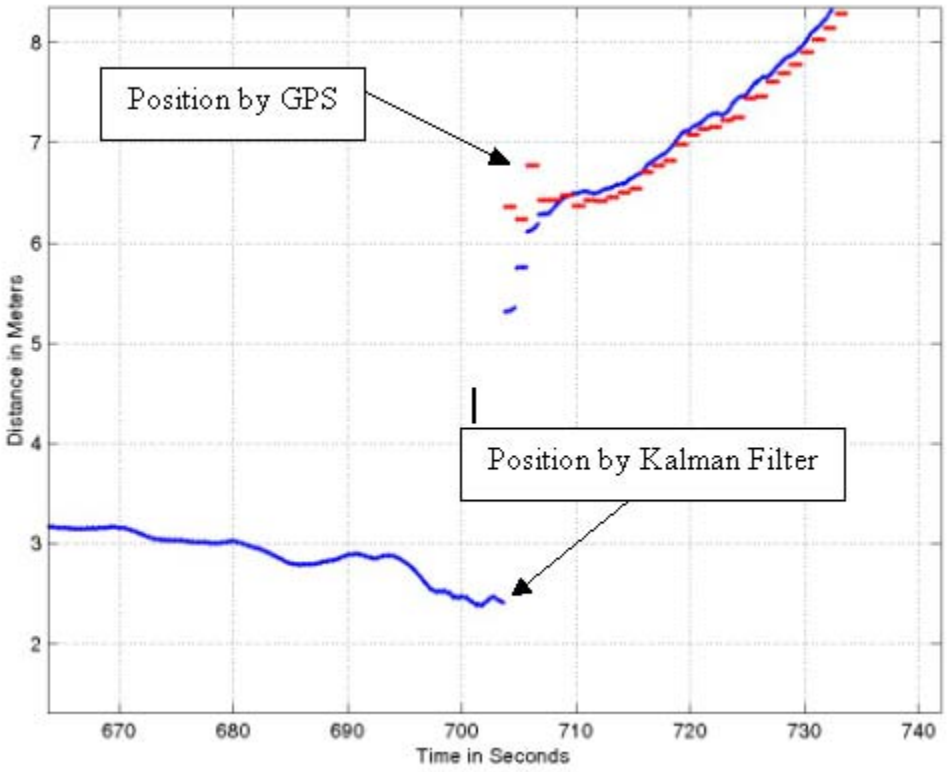

(b)

Figure 10. (a) Differences between GPS and Internal Navigation in the North Direction for the 3rd Surface on August 11, 2001 (b) Differences between GPS and Internal Navigation in the East/West Direction for the 3rd Surface on August 11, 2001.

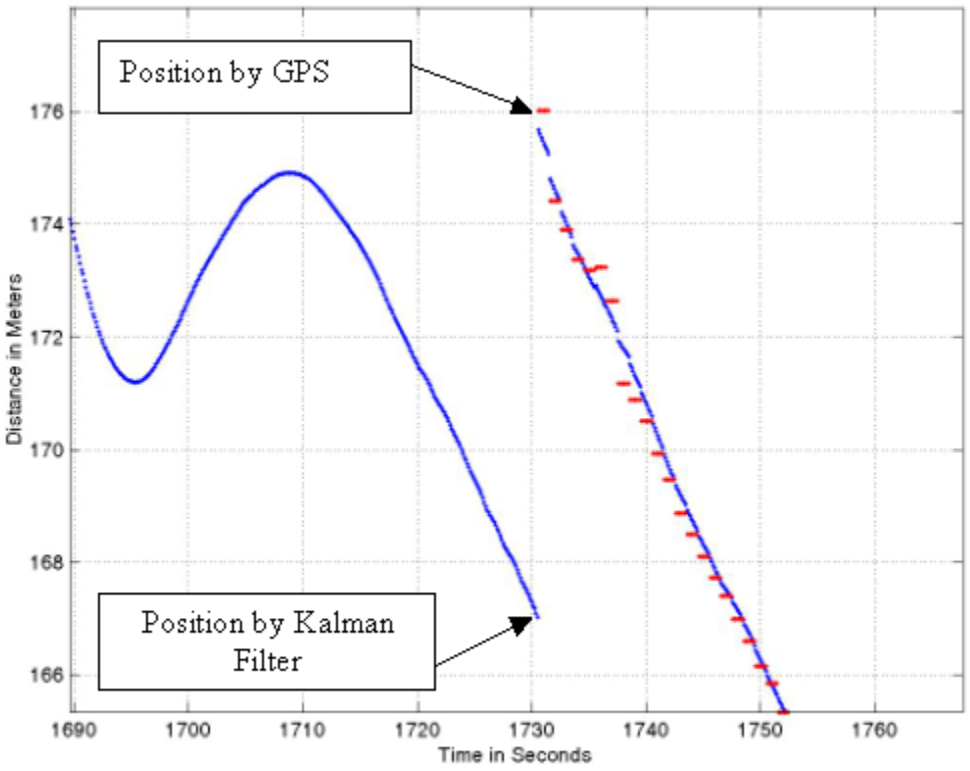
Position by GPS
Position by Kalman Filter
Distance in Meters
Time in Seconds
176
174
172
170
168
166
1690
1700
1710
1720
1730
1740
1750
1760

(a)

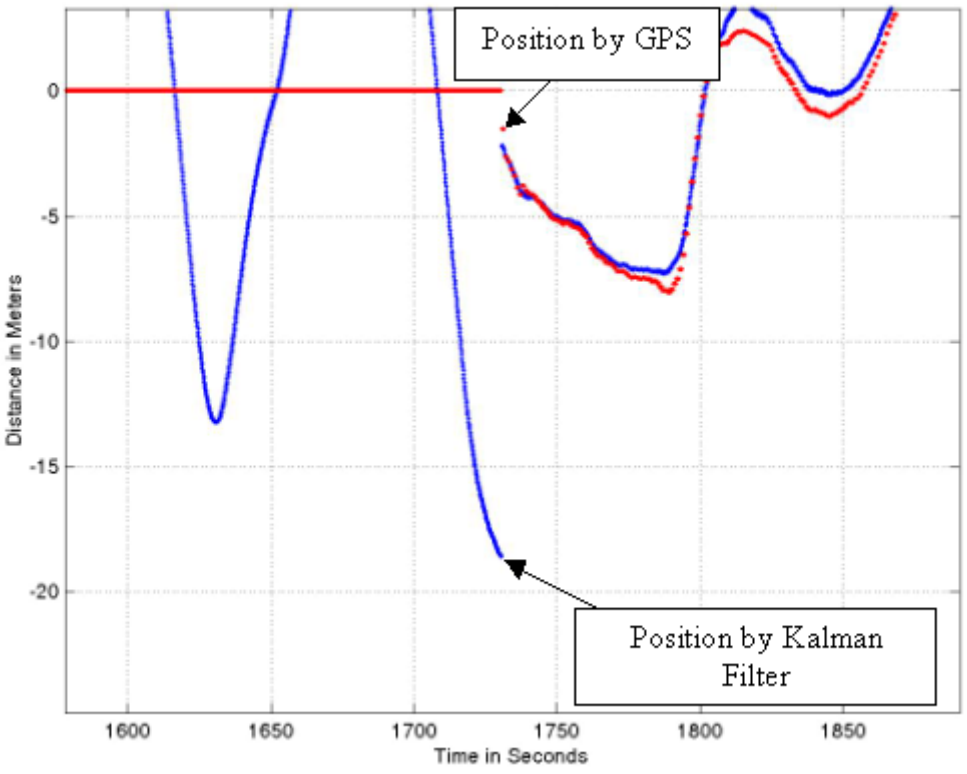

(b)

Figure 11. (a) Differences between GPS and Internal Navigation in the North Direction for the 4th Surface on August 11, 2001 (b) Differences between GPS and Internal Navigation in the East/West Direction for the 4th Surface on August 11, 2001.

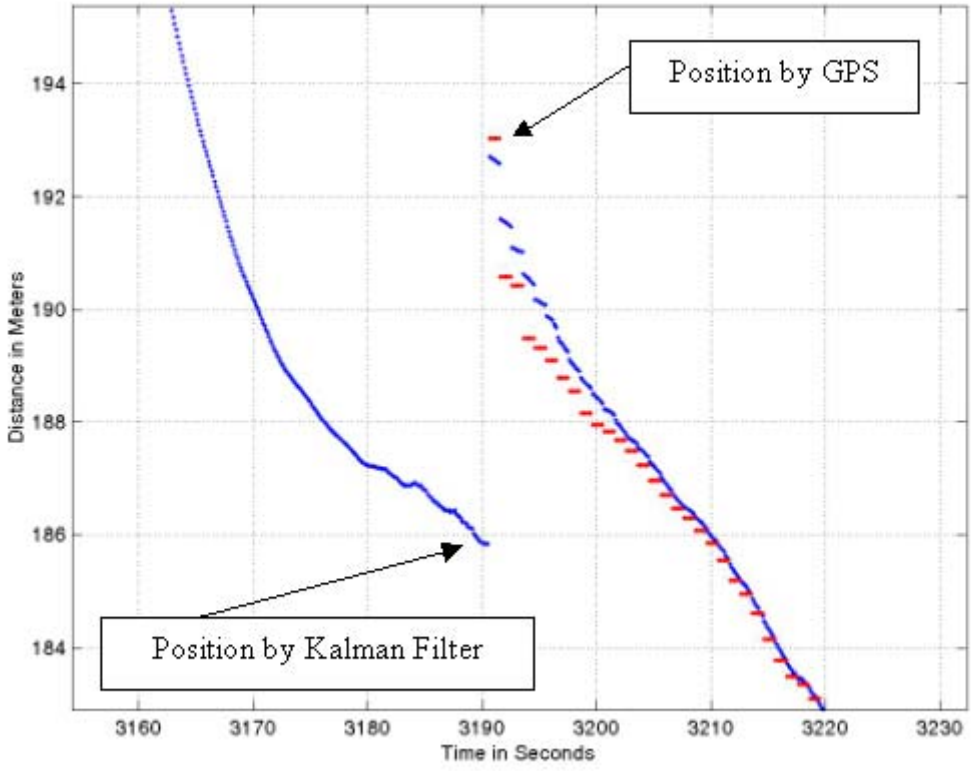
Position by GPS
Position by Kalman Filter
Distance in Meters
Time in Seconds
194
192
190
188
186
184
3160
3170
3180
3190
3200
3210
3220
3230

(a)

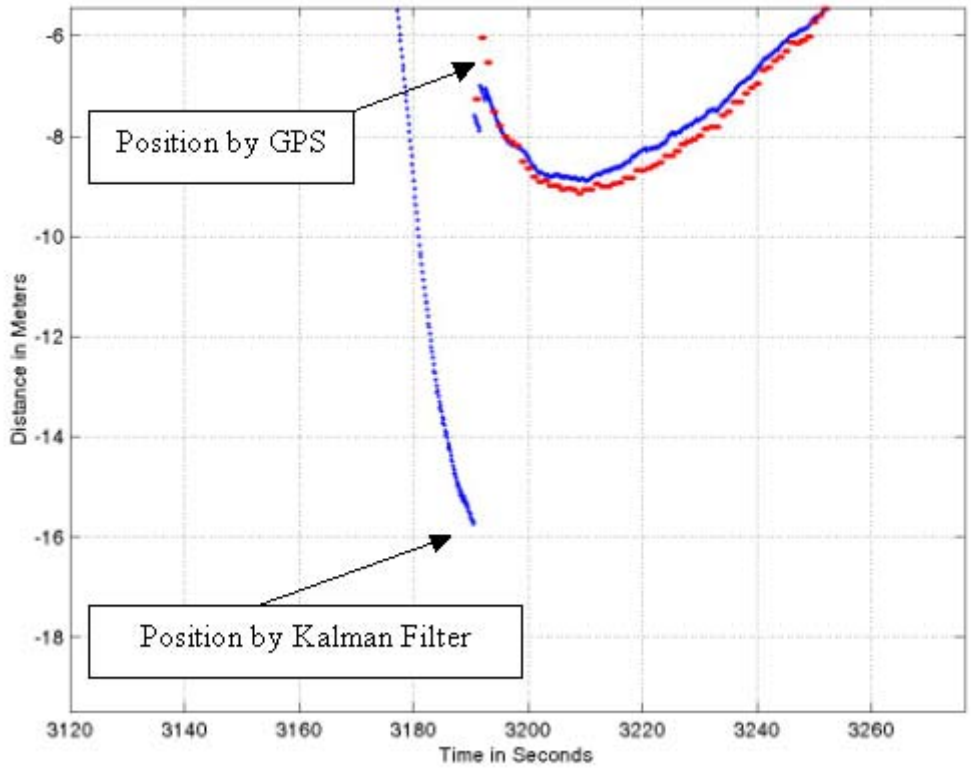

(b)

Figure 12. (a) Differences between GPS and Internal Navigation in the North Direction for the 5th Surface on August 11, 2001 (b) Differences between GPS and Internal Navigation in the East/West Direction for the 5th Surface on August 11, 2001.

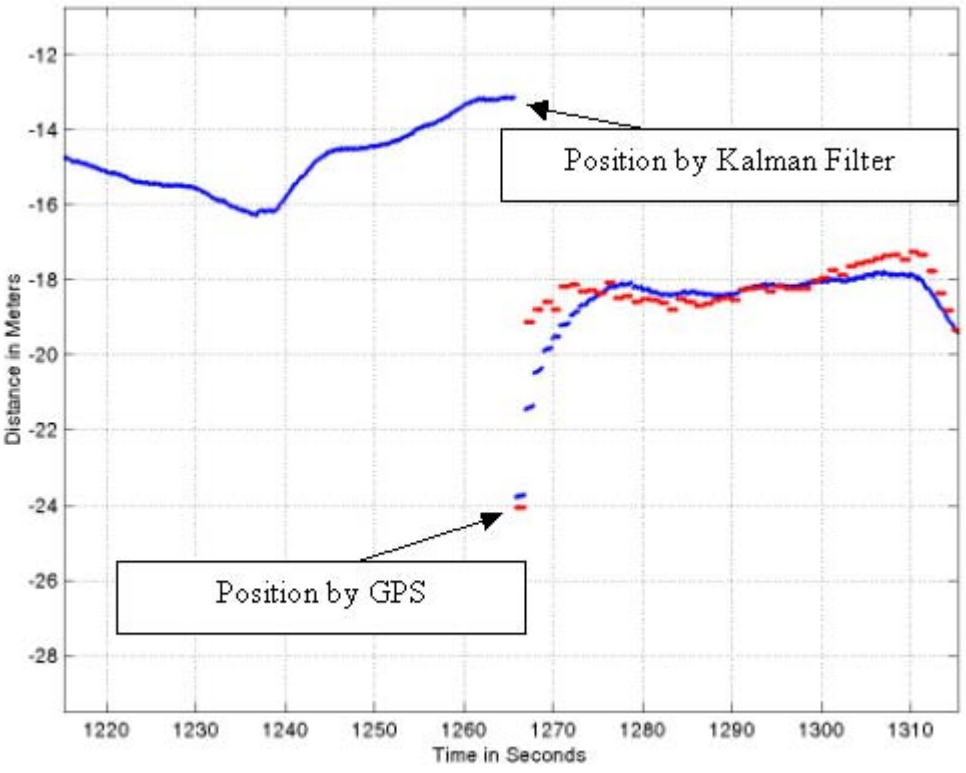
Position by Kalman Filter
Position by GPS
Distance in Meters
Time in Seconds
-12
-14
-16
-18
-20
-22
-24
-26
-28
1220
1230
1240
1250
1260
1270
1280
1290
1300
1310

(a)

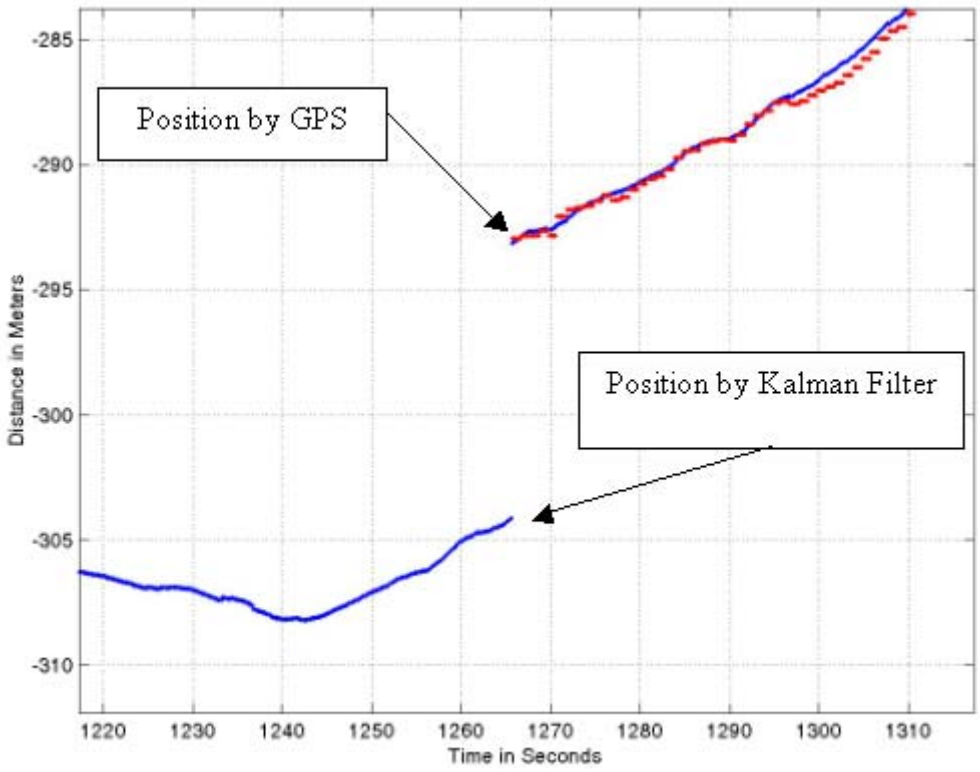

(b)

Figure 13. (a) Differences between GPS and Internal Navigation in the North Direction for the 6th Surface on August 11, 2001 (b) Differences between GPS and Internal Navigation in the East/West Direction for the 6th Surface on August 11, 2001.

For the mission run on August 12, 2001, data from seven dive-surface operations were extracted from the vehicle's internal file. Figures 14 through 20 compare vehicle locations obtained from GPS with locations calculated from the vehicle's internal navigation system. The differences in location are shown in meters in the Y-axis ant the time in second in the X-axis. Total submerged time for the AUV Aries varied between 36 to 427 seconds.

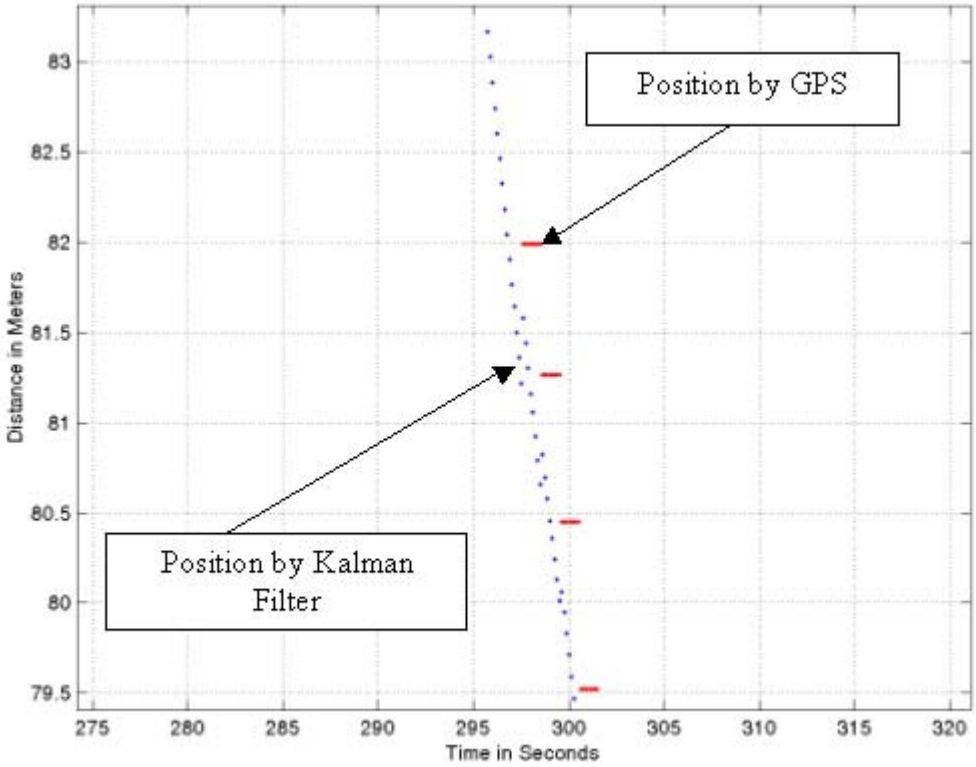

(a)

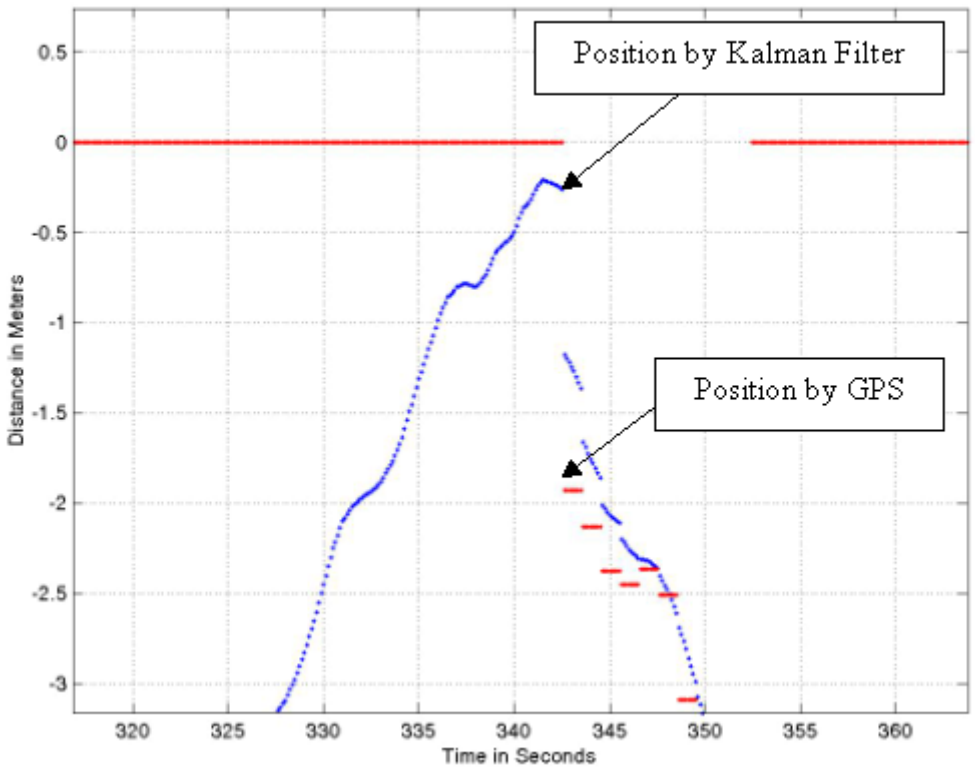

(b)

Figure 14. (a) Differences between GPS and Internal Navigation in the North Direction for the 1st Surface on August 12, 2001 (b) Differences between GPS and Internal Navigation in the East/West Direction for the 1st Surface on August 12, 2001.

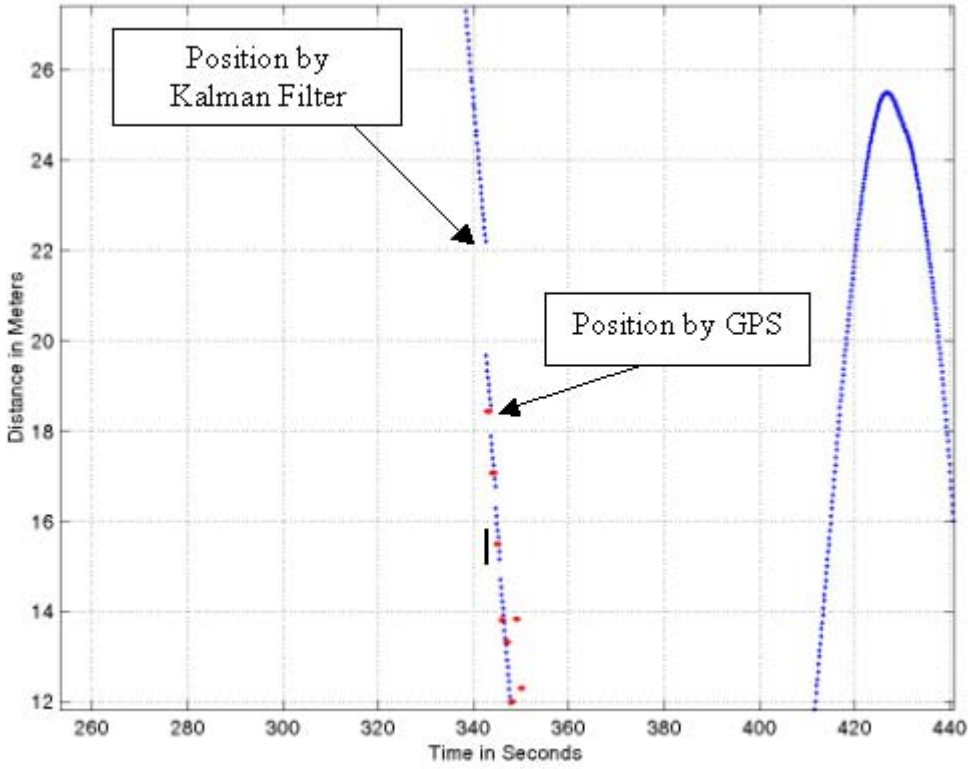
Position by
Kalman Filter
Position by GPS
Distance in Meters
Time in Seconds
26
24
22
20
18
16
14
12
260
280
300
320
340
360
380
400
420
440

(a)

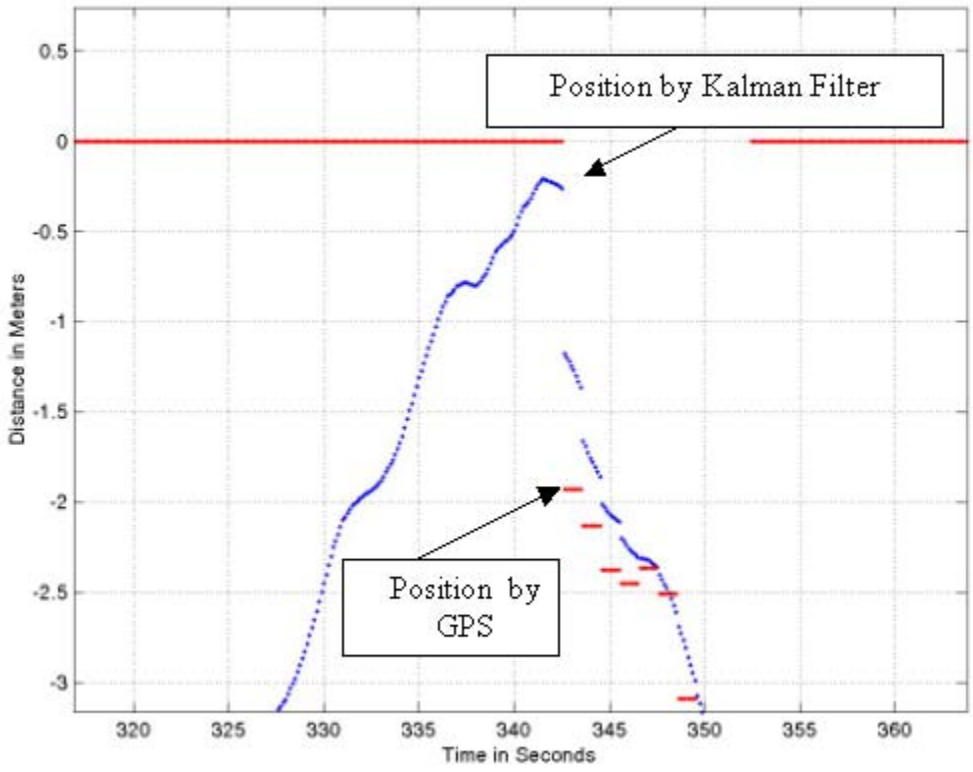

(b)

Figure 15. (a) Differences between GPS and Internal Navigation in the North Direction for the 2nd Surface on August 12, 2001 (b) Differences between GPS and Internal Navigation in the East/West Direction for the 2nd Surface on August 12, 2001.

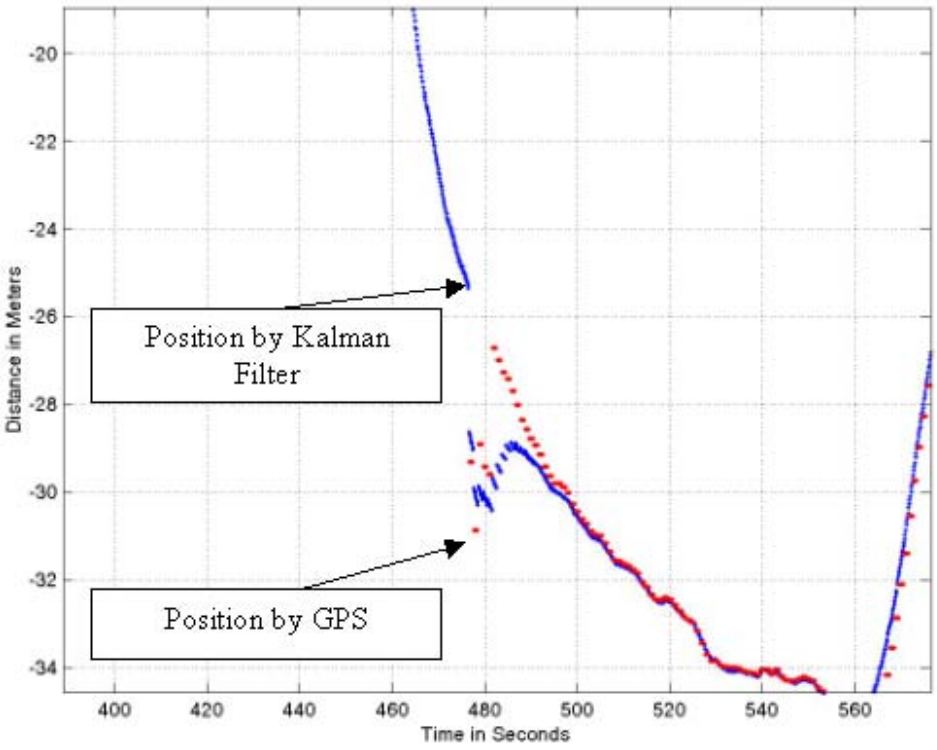
-20
-22
-24
-26
-28
-30
-32
-34
Distance in Meters
400
420
440
460
480
500
520
540
560
Time in Seconds
Position by Kalman Filter
Position by GPS

(a)

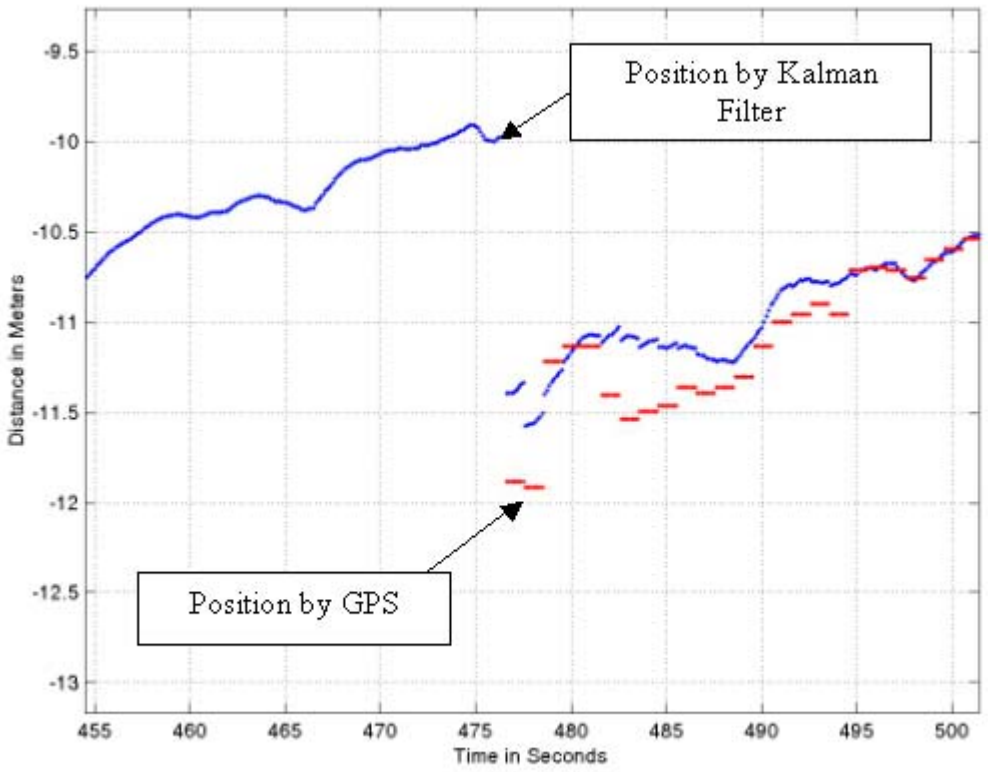

(b)

Figure 16. (a) Differences between GPS and Internal Navigation in the North Direction for the 3rd Surface on August 12, 2001 (b) Differences between GPS and Internal Navigation in the East/West Direction for the 3rd Surface on August 12, 2001.

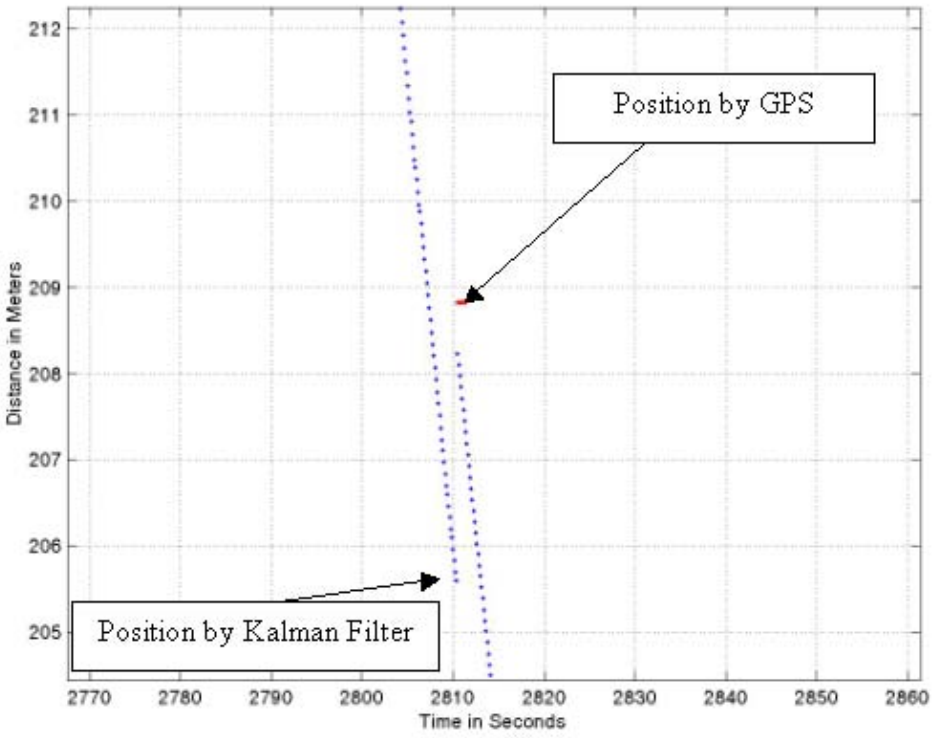
Position by GPS
Position by Kalman Filter
Distance in Meters
Time in Seconds
212
211
210
209
208
207
206
205
2770
2780
2790
2800
2810
2820
2830
2840
2850
2860

(a)

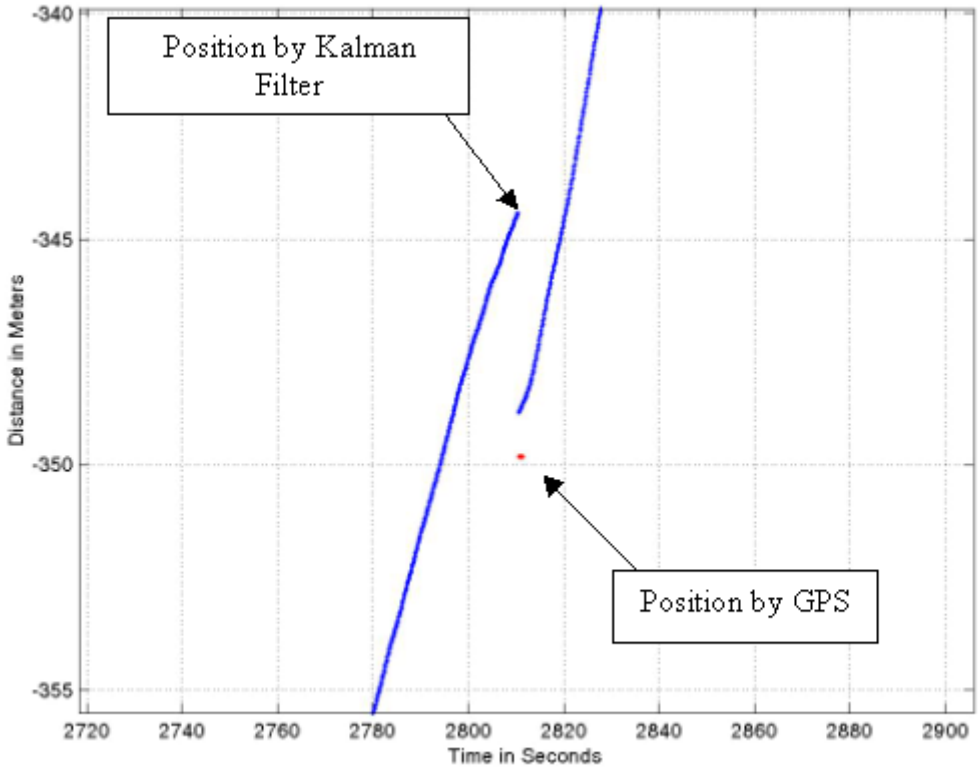

(b)

Figure 17. (a) Differences between GPS and Internal Navigation in the North Direction for the 4th Surface on August 12, 2001 (b) Differences between GPS and Internal Navigation in the East/West Direction for the 4th Surface on August 12, 2001.

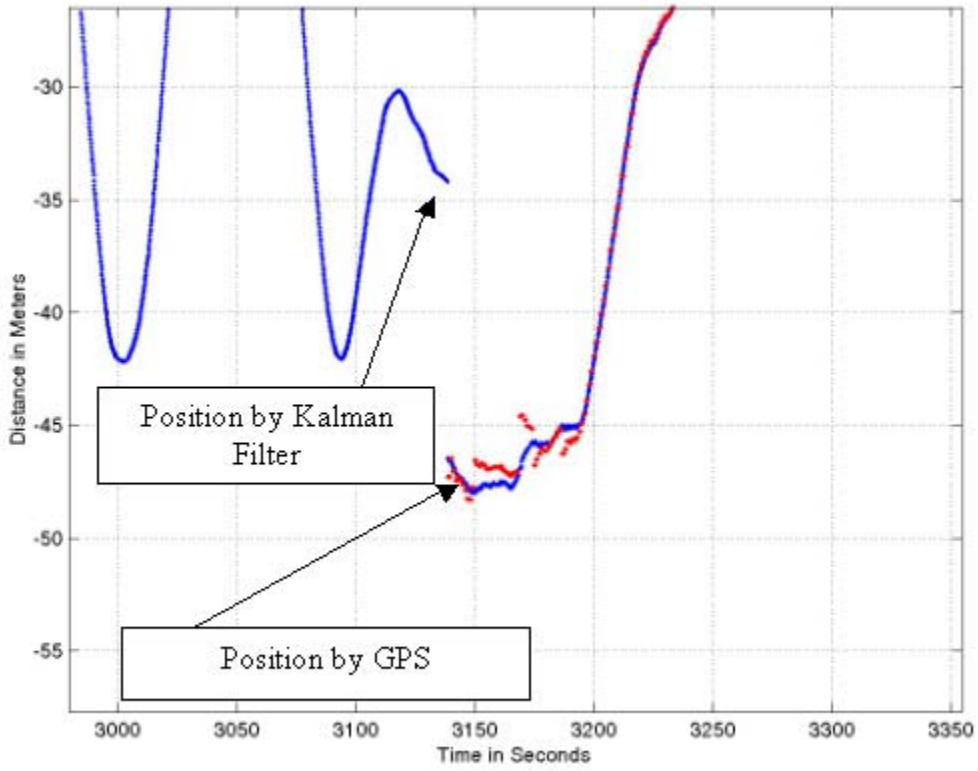
-30
-35
-40
-45
-50
-55
Distance in Meters
3000
3050
3100
3150
3200
3250
3300
3350
Time in Seconds
Position by Kalman Filter
Position by GPS

(a)

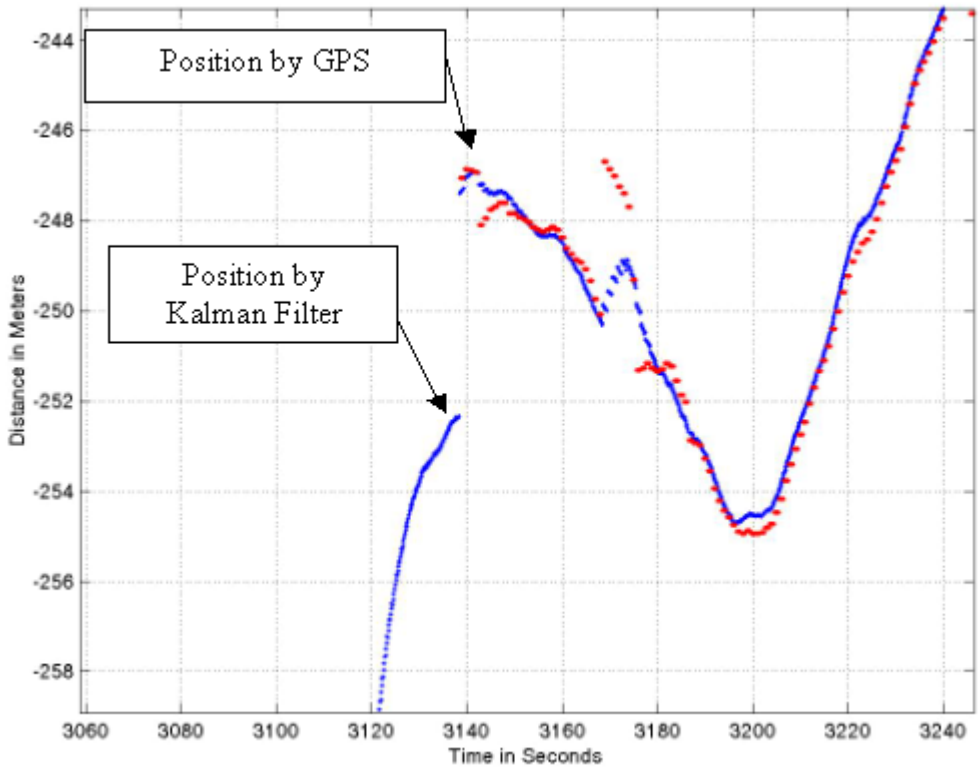

(b)

Figure 18. (a) Differences between GPS and Internal Navigation in the North Direction for the 5th Surface on August 12, 2001 (b) Differences between GPS and Internal Navigation in the East/West Direction for the 5th Surface on August 12, 2001.

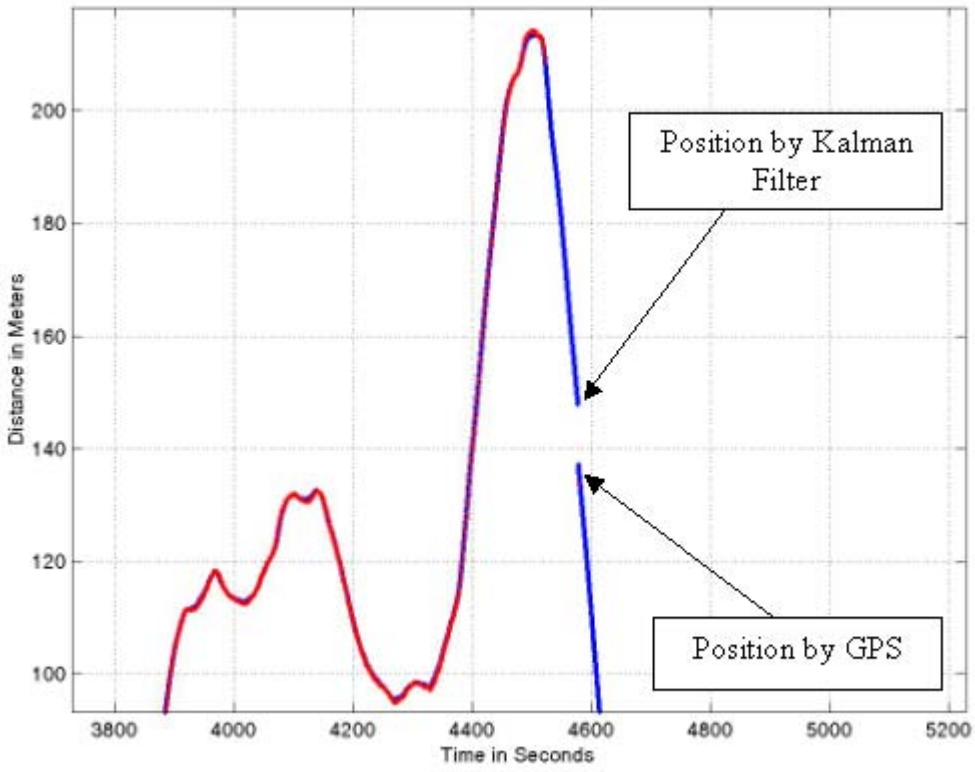
Position by Kalman Filter
Position by GPS
Distance in Meters
Time in Seconds
200
180
160
140
120
100
3800
4000
4200
4400
4600
4800
5000
5200

(a)

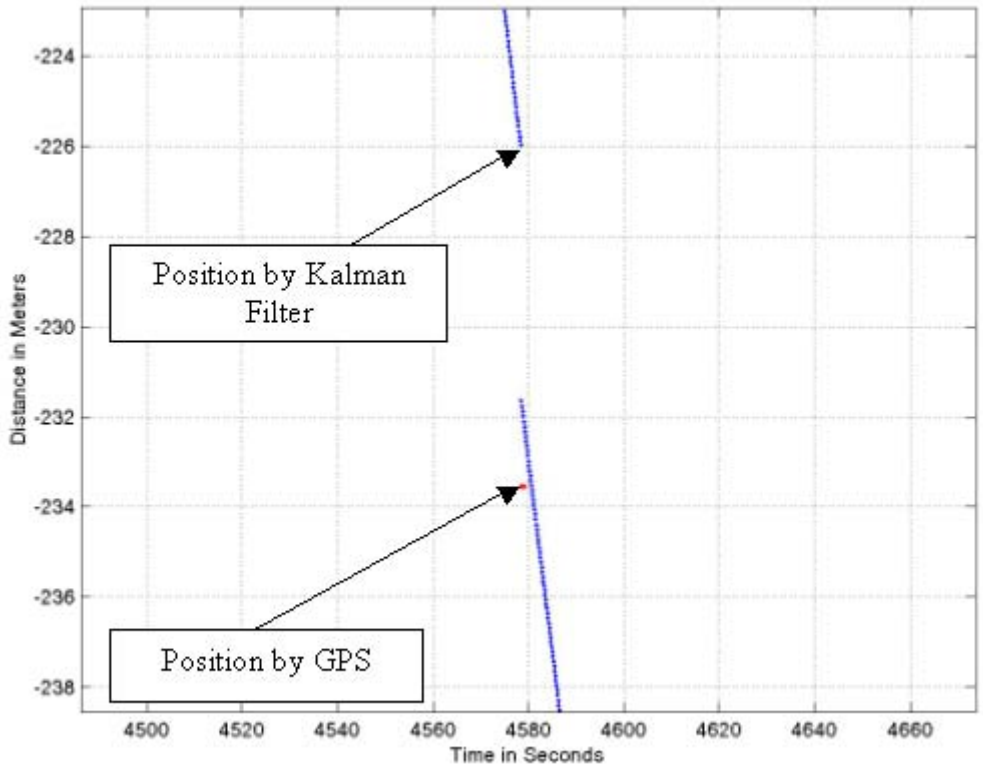

(b)

Figure 19. (a) Differences between GPS and Internal Navigation in the North Direction for the 6th Surface on August 12, 2001 (b) Differences between GPS and Internal Navigation in the East/West Direction for the 6th Surface on August 12, 2001.

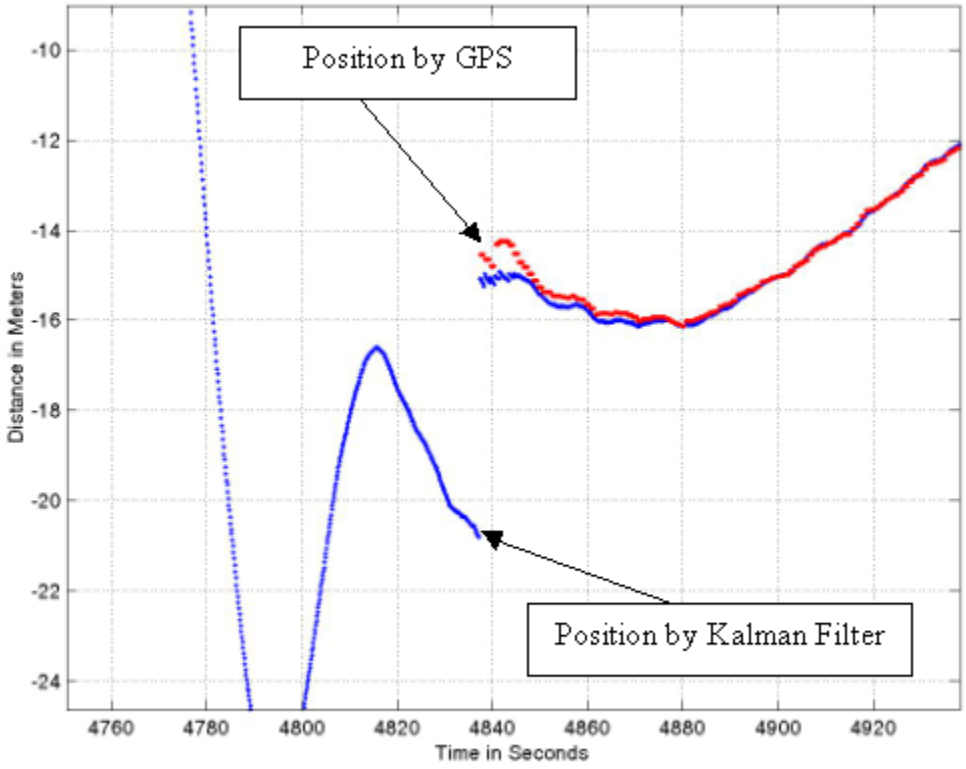
Position by GPS
Position by Kalman Filter
Distance in Meters
Time in Seconds
-10
-12
-14
-16
-18
-20
-22
-24
4760
4780
4800
4820
4840
4860
4880
4900
4920

(a)

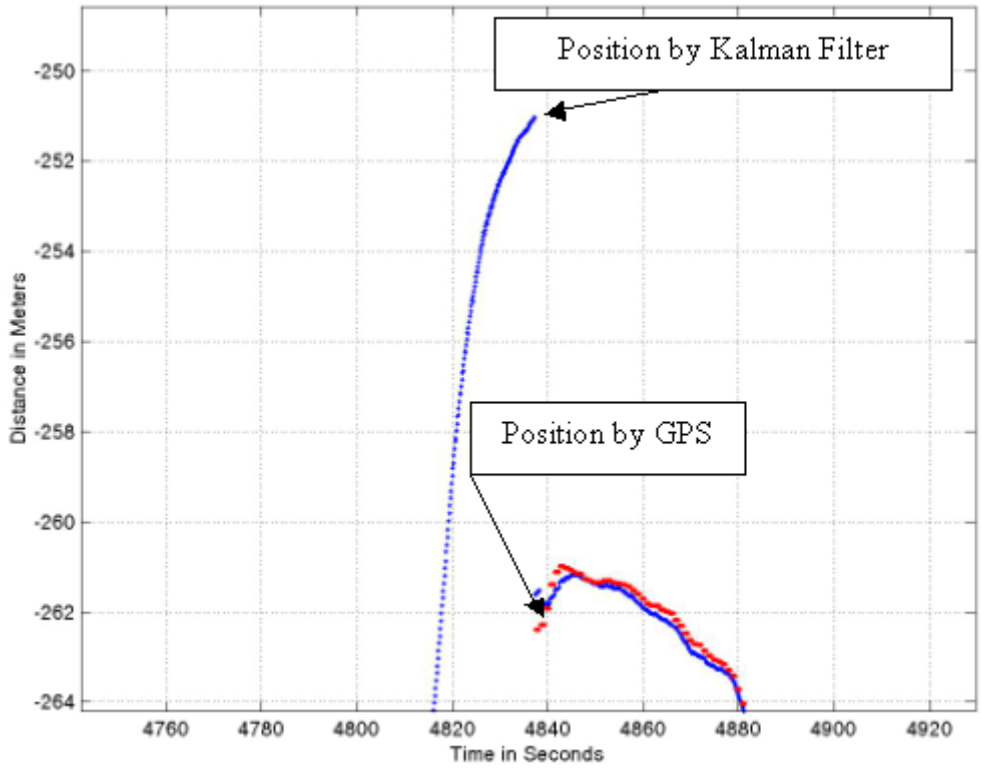

(b)

Figure 20. (a) Differences between GPS and Internal Navigation in the North Direction for the 7th Surface on August 12, 2001 (b) Differences between GPS and Internal Navigation in the East/West Direction for the 7th Surface on August 12, 2001.

Table 3 consolidates all thirteen dive surface operations and shows the total distance of track R.

Date	From	To	Total time vehicle submerged (seconds)	Y (m)	X (m)	R (m)	# of sat.	Hdop
08110102	311	398	87	2.0	0.2	**2.01**	6	1.4
	413	582	169	2.8	2.2	**3.56**	8	2.0
	596	703	107	4.0	13.0	**13.6**	3	7.6
	1237	1730	493	17.0	11.0	**20.25**	8	1.8
	2644	3190	546	9.8	7.2	**12.16**	8	3.1
08110104	839	1266	427	11.0	11.0	**15.56**	6	4.1
08120102	262	298	36	1.5	0.9	**1.75**	7	1.4
	306	343	37	1.7	4.0	**4.35**	6	6.9
	352	477	125	2.0	4.0	**4.97**	3	6.1
	2712	2811	99	5.3	3.2	**6.19**	4	8.3
	2811	3138	327	5.5	13.0	**14.12**	2	3.1
	4524	4578	54	7.5	14.0	**15.88**	3	8.2
	4578	4838	260	11.4	6.3	**13.02**	5	1.6

Table 3. Differences between GPS and Underwater Vehicle Navigation System during Surfaces from Aug 10-12, 2001.

The following three figures show that the position errors increase as the vehicle submersion time increases.

In Figure 21, a close up look at the difference between the Kalman filter solution and the DGPS data point in meters versus submerged time in seconds while AUV Aries surfaced for all thirteen dive-surface operations. The least square method was utilized to calculate the graph that best fitted all data points with the line going through the zero point origin. The MATLAB code for the least square method with the line going through the origin is listed in Appendix A.

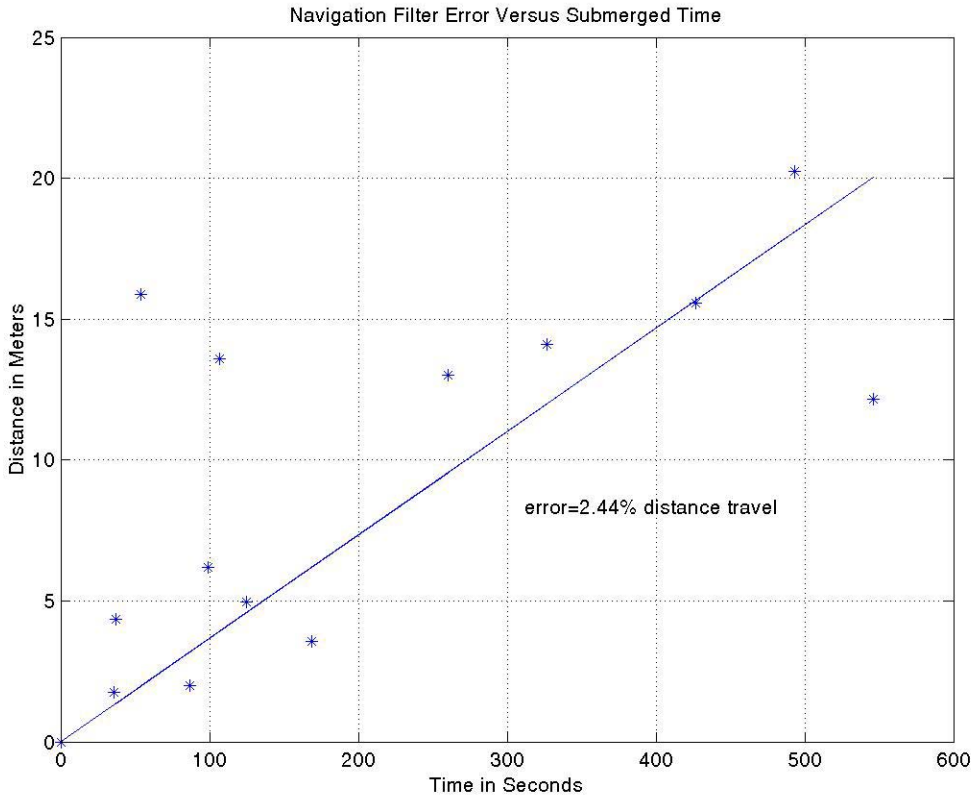

Figure 21. Difference between the Kalman Filter Solution and the DGPS Data Point in Meters Versus Submerged Time in Seconds.

In Figure 22, took into consideration that DGPS is more accurate if there were at least four satellites were being used to compute the position. Therefore, DGPS data with less four satellites were drop off. Again, the least square method was utilized to calculate the graph that best fitted all data points with the line going through the zero point origin. The MATLAB code for the least square method with the line going through the origin is listed in Appendix B.

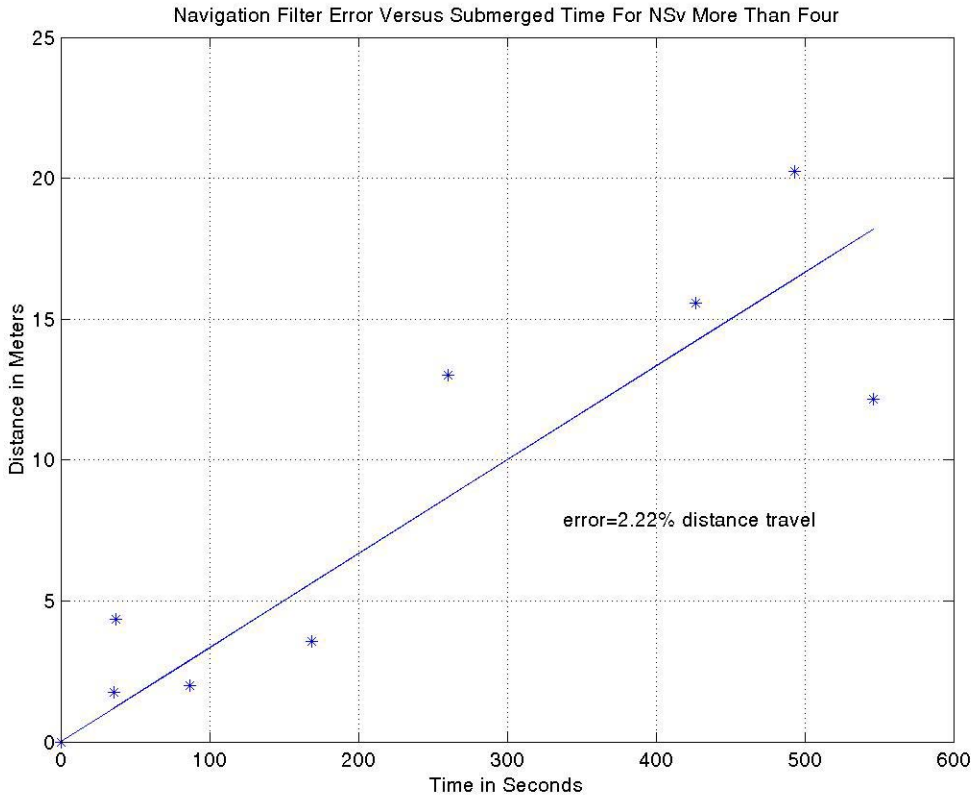

Figure 22. DGPS More Accurate with at least Four Satellites to Compute the Position.

In Figure 23, took into consideration of the Horizontal dilution of precision (Hdop) values. Values of Hdop between 1.2 and 1.7 are usually associated with high precision. This value is a good figure of merit. Therefore, DGPS data with a Hdop values of less than 1.2 or more than 2.0 were dropped off. Again, the least square method was utilized to calculate the graph that best fitted all data points with the line going through the zero point origin. The MATLAB code for the least square method with the line going through the origin is listed in Appendix C.

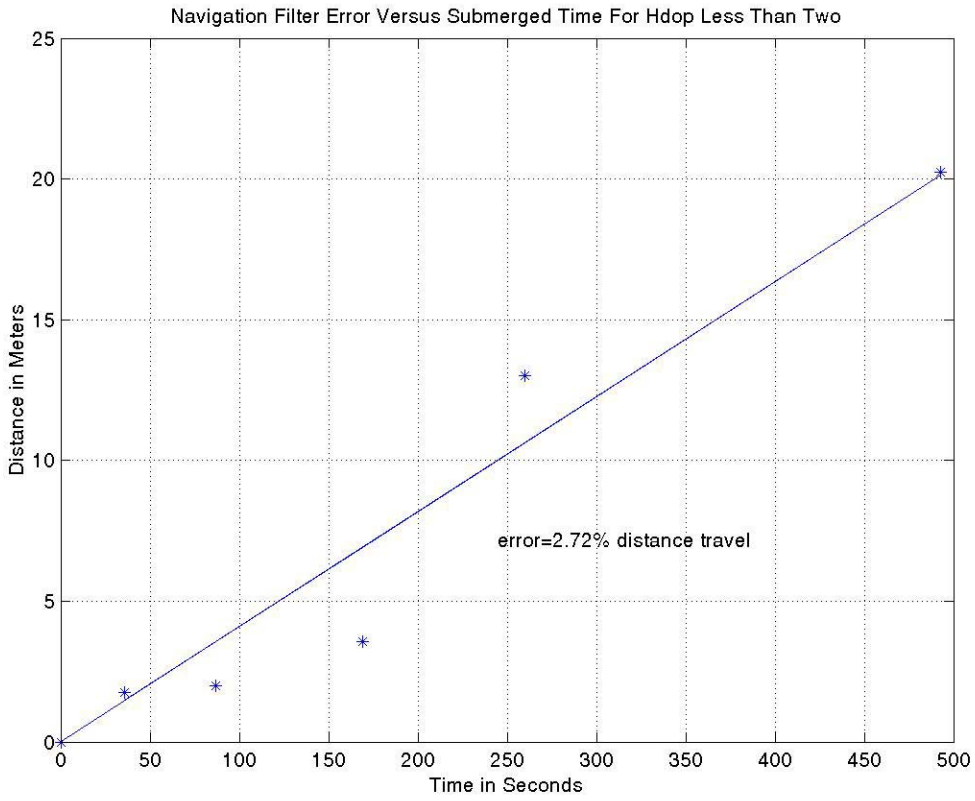

Figure 23. Horizontal Dilution of Precision (Hdop) Values.

B. TRACK FOLLOWING ALGORITHM

The AUV Aries currently uses four different automatic pilots for flight maneuvering control: diving, altitude above bottom, steering, and cross track error controllers [Ref. 1]. These four automatics pilots are based on sliding mode control theory. Each of the four modes is de-coupled for ease of implementation and design. [Ref. 7] provides the details of controller design. Sliding mode controllers are chosen over fuzzy and heuristic controllers because they are simple to use and implement with minimal tuning [Ref. 8].

1. Heading Controller

A second order model equation is used to control the vehicle heading and eliminates the need to feed back the sideslip velocity. The effects of sideslip are treated as disturbances that the controller must overcome. Therefore, the heading model equation becomes:

$$\dot{r}(t) = ar(t) + b\delta_r(t) + disturbances \tag{1}$$

$$\dot{\psi}(t) = r(t) \tag{2}$$

where $\psi(t)$ is the vehicle heading angle, $r(t)$ is the yaw rate, and $\delta_r(t)$ is the stern rudder angle. The coefficients, a and b, have been determined from experiments; and they are -.30/sec and -.1125/sec^2 respectively. The stern and bow rudders operate in the same way as the planes, therefore, the command to the bow rudder is $-\delta_r(t)$. In order to use this steering law, the heading error $(\psi_{com} - \psi(t))$ must lie between $\pm 180^0$ and is de-wrapped as needed in order to make this happen. By ignoring any non-zero command, the sliding surface is defined by

$$\sigma(t) = -.9499r(t) + .1701(\psi_{com} - \psi(t)) \tag{3}$$

The stern rudder command for heading control is defined by

$$\delta_t(t) = -1.543(2.5394r(t) + \eta \tanh(\sigma(t)/\phi)) \tag{4}$$

where η=1.0 and ϕ=0.5.

2. Cross Track Error Controller

To follow a set of predicted straight line tracks from a simulation model of the vehicle track following behavior [Ref. 1], a sliding mode controller is presented that has been experimentally validated. Other works have been studied for this type of problem [Ref. 9] usually developing a stable guidance law based on cross track error. Utilizing Figure 24 as a guide, we use a combination of cross track error control and line of sight control. Cross track error control cannot be guaranteed stable with large error heading, while line of sight control will reduce heading errors to zero. Switching between these two controllers allows for stable control and reduction in heading errors under all conditions.

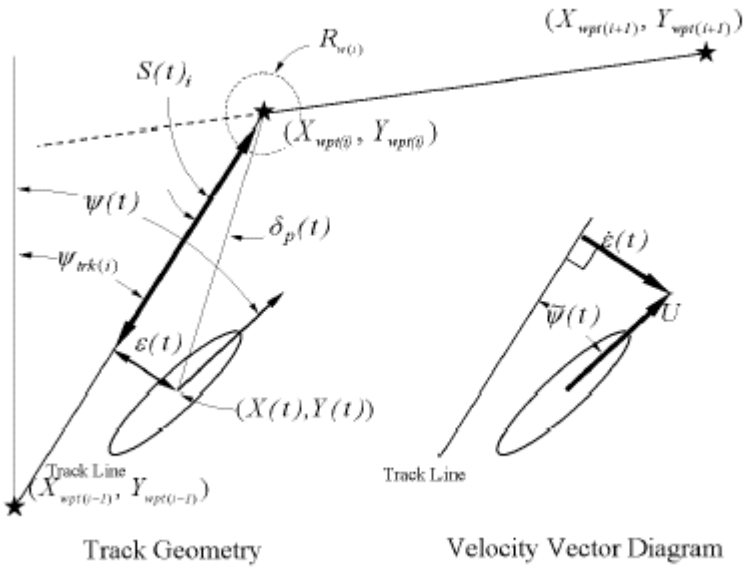

Figure 24. Track Geometry and Velocity Vector Diagram.

The variable of interest to minimize is the cross track error, $\varepsilon(t)$, and is defined as the perpendicular distance between the center of the vehicle located at $X(t), Y(t)$ and the adjacent track line. The total track length between way point i and $i-1$ is given by

$$L_i = \sqrt{(X_{wpt(i)} - X_{wpt(i-1)})^2 + (Y_{wpt(i)} - Y_{wpt(i-1)})^2} \tag{5}$$

where the pairs $X_{wpt(i)}, Y_{wpt(i)}$ and $X_{wpt(i-1)}, Y_{wpt(i-1)}$ are the current and previous way points respectively. The track angle, $\psi_{trk(i)}$, is defined by

$$\psi_{trk(i)} = \arctan 2(Y_{wpt(i)} - Y_{wpt(i-1)}, X_{wpt(i)} - X_{wpt(i-1)}) \tag{6}$$

and is constant for a given set of adjacent way points. Cross track heading error, $\bar{\psi}(t)_{cte(i)}$, for the i^{th} segment is defined by

$$\bar{\psi}(t)_{cte(i)} = \psi(t) - \psi_{trk(i)} \tag{7}$$

where $\bar{\psi}(t)_{cte(i)}$ must be normalized to stay between $\pm 180^o$. The difference between the current vehicle position and the next waypoint is

$$\begin{aligned} \overset{\square}{X}(t)_{wpt(i)} &= X_{wpt(i)} - X(t) \\ \overset{\square}{Y}(t)_{wpt(i)} &= Y_{wpt(i)} - Y(t) \end{aligned} \tag{8}$$

With the above definition, the distance to the i^{th} way point projected to the track line, $S(t)$ can be defined as

$$S(t)_i = [\overset{\square}{X}(t)_{wpt(i)} \overset{\square}{Y}(t)_{wpt(i)}].[(X_{wpt(i)} - X_{wpt(i-1)})(Y_{wpt(i)} - Y_{wpt(i-1)})]/L_i \ . \tag{9}$$

$S(t)$ ranges from 0-100% of L_i

The cross track error, $\varepsilon(t)$, may now be defined as

$$\varepsilon(t) = S(t)_i \sin(d_p(t)) \tag{10}$$

where $d_p(t)$ is the angle between the line of sight to the next way point and the current track line, given by

$$d_p(t) = \arctan 2(Y_{wpt(i)} - Y_{wpt(i-1)}, X_{wpt(i)} - X_{wpt(i-1)}) - \arctan 2(\overset{\square}{Y}(t)_{wpt(i)}, \overset{\square}{X}(t)_{wpt(i)}) \ . \tag{11}$$

and $d_p(t)$ must be normalized to lie between $\pm 180^0$, and arctan2 is the inverse tangent function atan2, as defined in MATLAB language.

With the cross track error defined, the sliding surface can be cast in terms of derivatives of the errors such that.

$$\dot{\varepsilon}(t) = U \sin(\overset{\approx}{\psi}(t)_{cte(i)})$$

$$\ddot{\varepsilon}(t) = Ur(t) \cos(\overset{\approx}{\omega}(t)_{cte}) \qquad\qquad 0 \langle \overset{\approx}{\omega}(t)_{cte(i)} \langle pi/2;$$

$$\dddot{\varepsilon}(t) = U\dot{r}(t) \cos(\overset{\approx}{\omega}(t)_{cte}) - Ur(t)^2 \sin(\overset{\approx}{\omega}(t)_{cte(i)})$$

where U is the nominal longitudinal speed of the vehicle. The sliding surface for the cross track error controller becomes a second order polynomial of the form

$$\sigma(t) = \ddot{\varepsilon}(t) + \lambda_1 \dot{\varepsilon}(t) + \lambda_2 \varepsilon(t) \tag{12}$$

The condition for stability of the sliding mode controller is

$$\dot{\sigma}(t) = \dddot{\varepsilon}(t) + \lambda_1 \ddot{\varepsilon}(t) + \lambda_2 \dot{\varepsilon}(t) = -\eta(\sigma(t)/\varphi), \tag{13}$$

and to recover the input for control, the heading dynamics, equation (1), may be used into equation (12) to yield

$$U(ar(t)+b\delta_r(t))\cos(\tilde{\omega})_{cte}) - Ur(t)^2 \sin(\tilde{\omega}(t)_{cte(i)}) + \lambda_1 Ur(t)\cos(\tilde{\omega}(t)_{cte(i)}) + \lambda_2 U\sin(\tilde{\omega}(t)_{cte(i)}) = -\eta(\sigma(t)/\varphi);$$
$$0\langle \tilde{\omega}(t)_{cte(i)} \langle pi/2; \tag{14}$$

By rewriting equation (12), the sliding surface becomes

$$\sigma(t) = Ur(t)\cos(\tilde{\omega}(t)_{cte(i)}) + \lambda_1 U\sin(\tilde{\omega}(t)_{cte(i)}) + \lambda_2 \varepsilon(t). \tag{15}$$

the rudder input can be expressed as

$$\delta_r(t) = \left(\frac{1}{Ub\cos(\tilde{\omega}(t)_{cte(i)})}\right)(-Uar(t)\cos(\tilde{\omega}(t)_{cte(i)}) + U(r(t))^2 \sin(\tilde{\omega}(t)_{cte(i)}) - \lambda_1 Ur(t)\cos(\tilde{\omega}(t)_{cte(i)})$$
$$-\lambda_2 U\sin(\tilde{\omega}(t)_{cte(i)} - \eta(\sigma(t)/\varphi)); \tag{16}$$

where λ_1=0.6, λ_2=0.1, η=0.1, and φ=0.5. To avoid division by zero, in the rare case where $\cos(\tilde{\omega}(t)_{cte(i)}) = 0$ (vehicle heading is perpendicular to the track line) the rudder command is set to zero since this condition is transient in nature. If $\tilde{\omega}(t)_{cte(i)} \langle pi/2$, then the vehicle will follow the track, but travel in the opposite direction to that desired. In order to prevent this from happening in practice, a bound of 40 degrees is used as a switch to light of sight control.

3. Line of Sight Controller

When the condition arises that the magnitude of the cross track heading error exceeds 40 degrees, a line of sight is used and the heading command can be determined from

$$\psi(t)_{com(LOS)} = \arctan 2(\tilde{Y}(t)_{wpt(i)}, \tilde{X}(t)_{wpt(i)}), \quad (17)$$

and the line of sight error from

$$\tilde{\psi}(t)_{LOS} = \psi(t)_{com(LOS)} - \psi(t) \quad (18)$$

The laws used for heading control, equations (3, 4), may be used. When the mission begins, the initial heading of the vehicle is seldom aligned with the command track. Line of sight control forces the vehicle to head in the direction of the current way point and once the cross track heading error falls below 40 degrees, cross track control is used. In the second scenario, when the angle between two sequential tracks lines exceeded 40 degrees, two conditions may be true for the waypoint index to be incremented. The first would be if the vehicle has penetrated the waypoint watch radius, R, which is set at 2 meters for this track following model. The second would be if a large amount of cross track error is presented. In that case, the next way point would become active if the projected distance to the way point, $S(t)_i$, reached $S_{\min(i)}$, such that if $(\sqrt{(\tilde{X},(t)_{wpt(i)})^2 + (\tilde{X}(t)_{wpt(i)})^2} \le R_{w(i)}, or, S(t)_i < S_{\min(t)}$ then activate the next way point.

C. COMPARISON OF DESIGN TRACKS, MODEL PREDICTION TRACKS AND ACTUAL TRACKS

Using the track prediction program called New-CTE-Box pattern, a box search pattern was used to circle the predicted autonomous underwater vehicle target points. The MATLAB code for the New-CTE-Box pattern is included as Appendix D. Twenty-four track lengths and twenty-four turning points were entered into the model prediction tracks program. The twenty-four points are a result of a model AUV Aries running in the same square box pattern six times. The same preprogrammed tracks and turning points were also loaded into the AUV Aries during the mission runs in the Azores on August 10-12, 2001. However, the AUV Aries executed only twelve track lengths and twelve tuning points, which is equivalent to running the same square box pattern three times. Data collected from the mission were stored and loaded into the track prediction program as experimental values of the actual tracks. Simulations of the AUV Aries run was performed by the prediction program based on similar conditions. Figure 25 shows the

differences in the design tracks, model prediction tracks and actual tracks. Analysis and comparison show that the actual tracks differ from the design tracks by margins of between 2 to 15 meters. This error is due, among other reasons, to rudder response time, forward motion, sway, yaw, cross track error steering and line of sight steering. Like an automobile, it is impossible for the AUV Aries to turn a 90 degrees corner while in continuous motion. The prediction tracks and the actual tracks are very similar in shape. The differences between actual tracks and prediction tracks (2 to 4 meters) are smaller than the differences between actual and design tracks. More importantly, model tracks reach a steady state after the first loop. This convergence demonstrates that the prediction program works. At the very end of the run, the AUV Aries aborted and surfaced. The prediction program does not simulate the end of the run where the AUV Aries finished and surfaced.

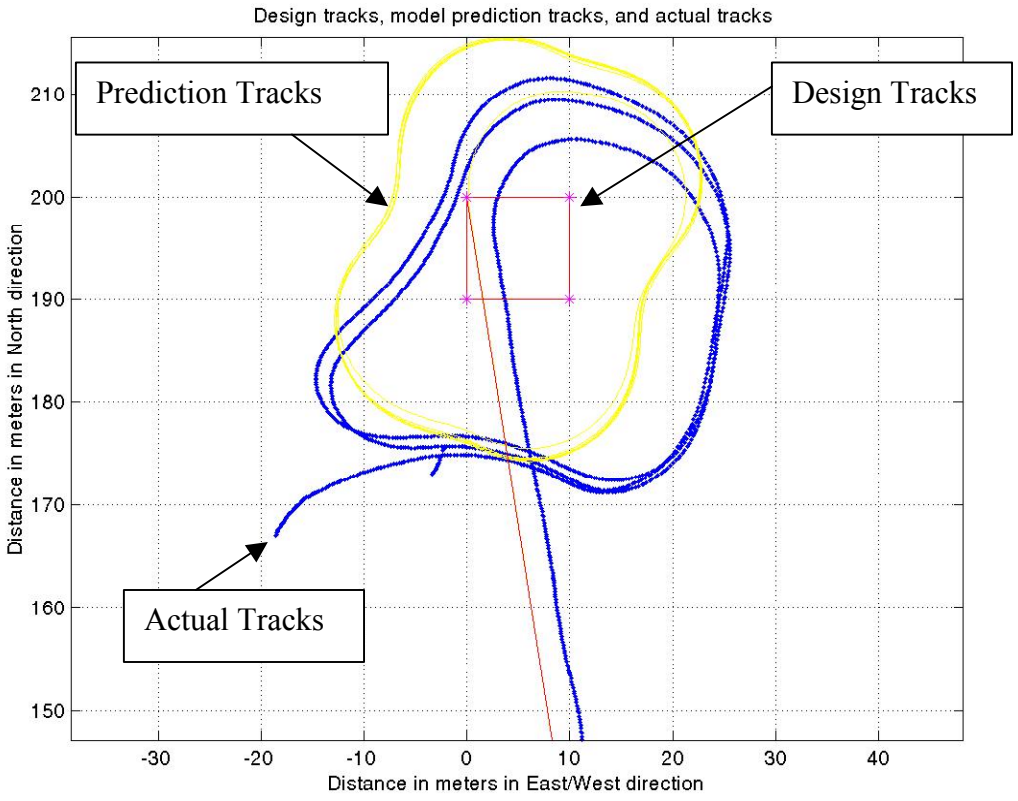

Figure 25. Design Tracks, Model Prediction Track and Actual Tracks with Simulated No Current.

Figure 26, utilizing the same actual tracks and design tracks, introduces a simulated current in the south direction at 0.5 knots for the prediction model. The design tracks and actual tracks remain the same as in Figure 25. However, the model prediction tracks reached steady state and are closer to the actual tracks. This indicates that the ocean current was in the southern direction during the mission run.

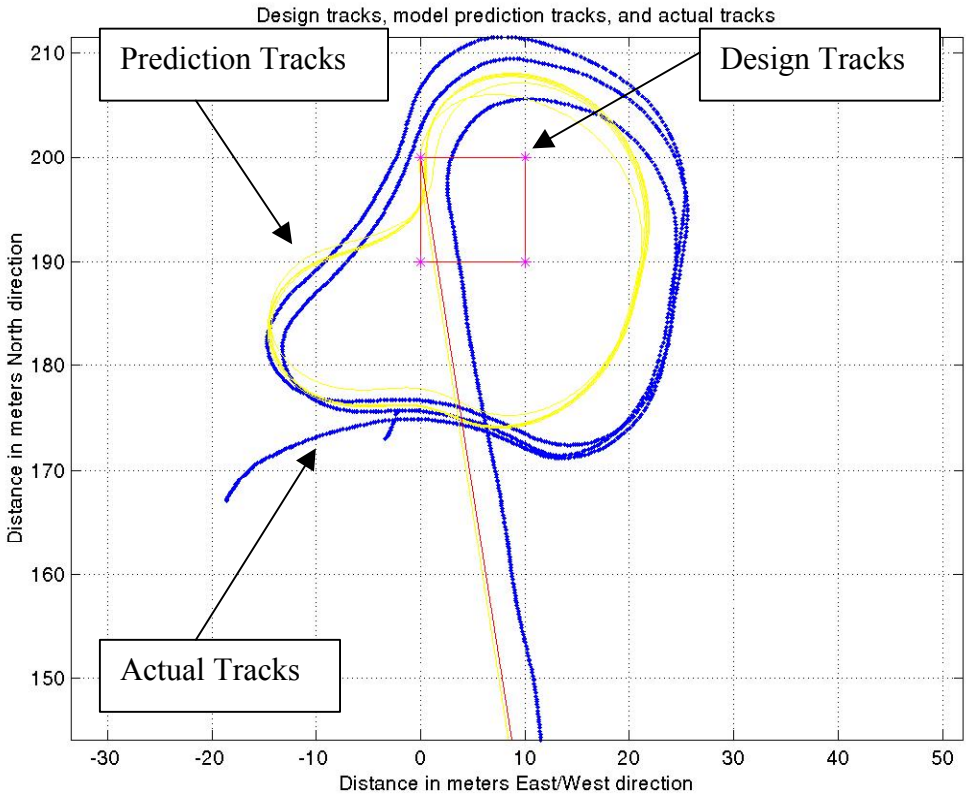

Figure 26. Design Tracks, Model Prediction Track and Actual Tracks with Simulated South Current.

Figure 27 introduces a simulated current in the north direction at 0.5 knots. The design tracks and actual tracks remain the same. The prediction tracks reached a steady state but were shifted in the direction of the current, and thus increased the separation between the actual tracks and the prediction tracks. This further indicates that the current was in the southern direction at the time of the mission run.

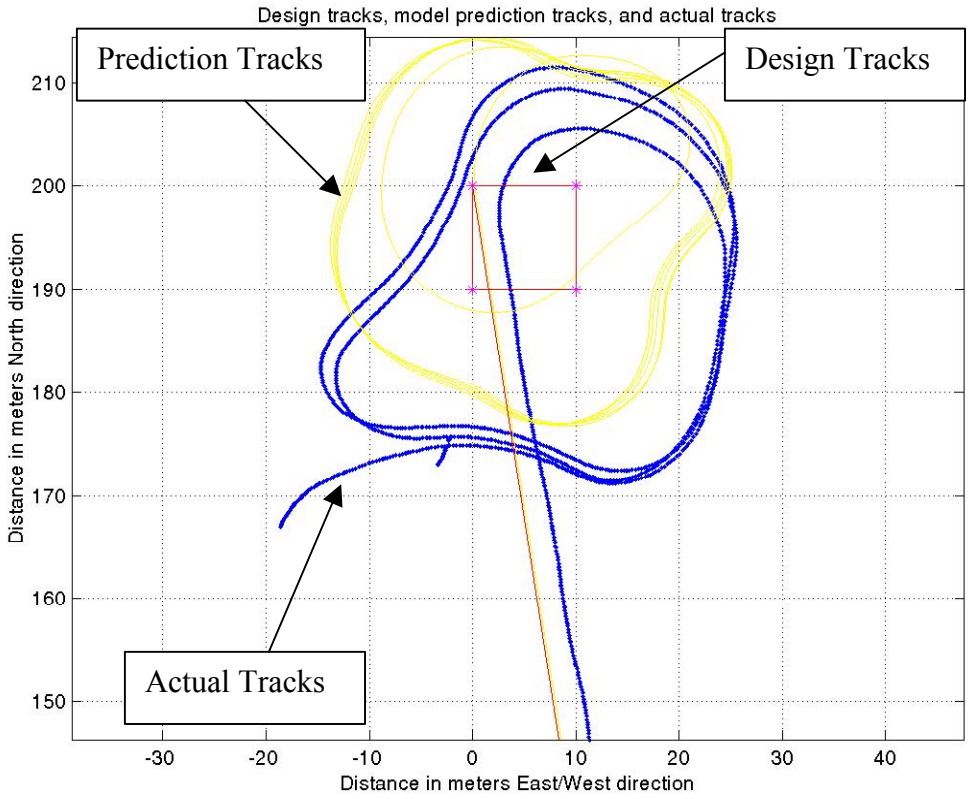

Figure 27. Design Tracks, Model Prediction Track and Actual Tracks with Simulated North Current.

Figure 28 introduces a simulated current in the east direction at 0.5 knots. The prediction tracks reached a steady state and are closer to the actual tracks. This indicates that the ocean current was in the easterly direction during the mission run.

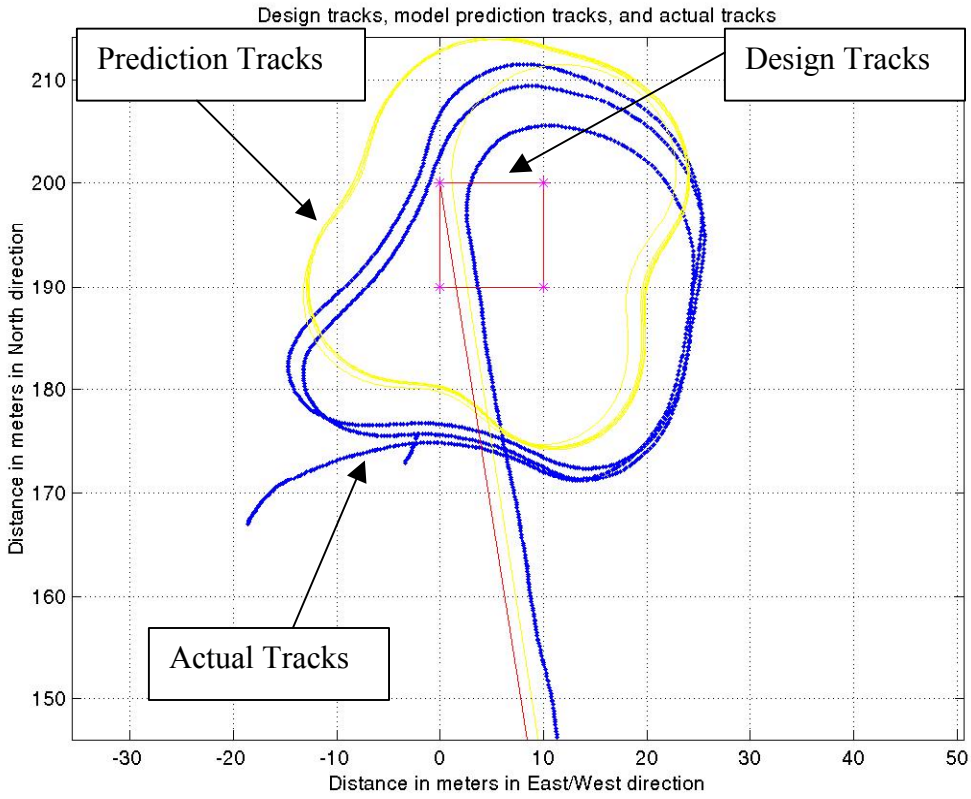

Figure 28. Design Tracks, Model Prediction Track and Actual Tracks with Simulated East Current.

Lastly, Figure 29 introduces a simulated current in the west direction at 0.5 knots. The actual tracks and designed tracks remain unchanged. The prediction tracks reached a steady state but were shifted in the direction of the current, which increased the separation between the actual tracks and the prediction tracks. This also indicated that the direction of the ocean current was in the easterly direction. Based on these four imposed current conditions, it was determined that the direction of the current was somewhere in the southeast direction.

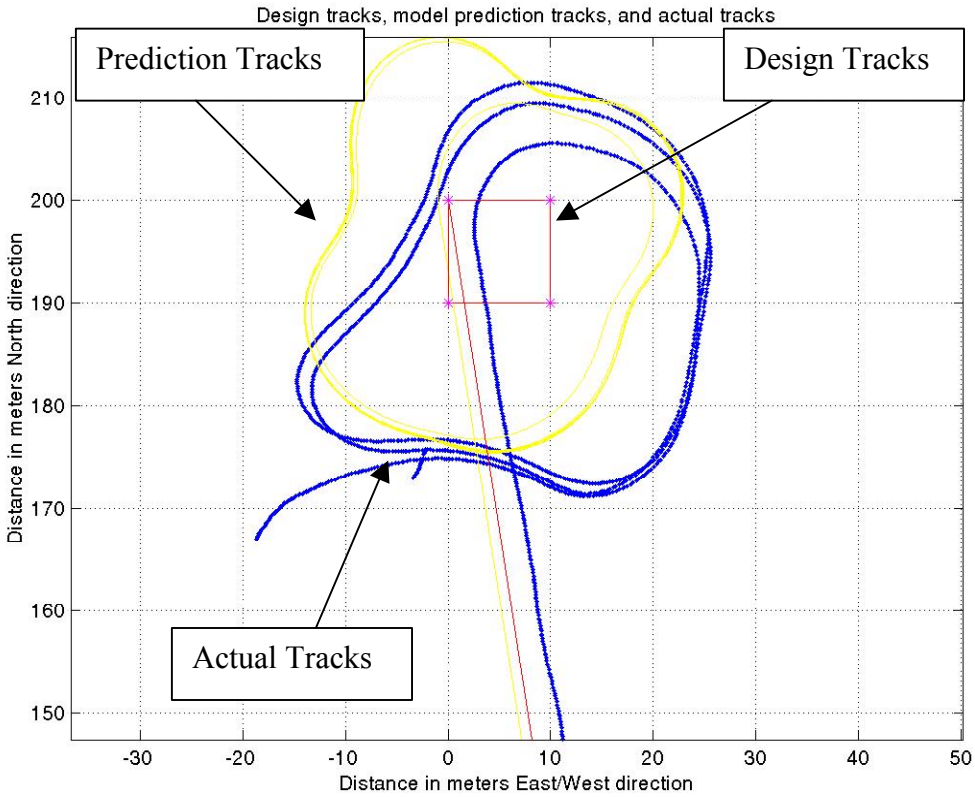

Figure 29. Design Tracks, Model Prediction Track and Actual Tracks with Simulated West Current.

Figure 30 shows a current of 0.5 knots in the south and 0.5 knots in the east. The prediction tracks again reached a steady state and are very close to the actual tracks.

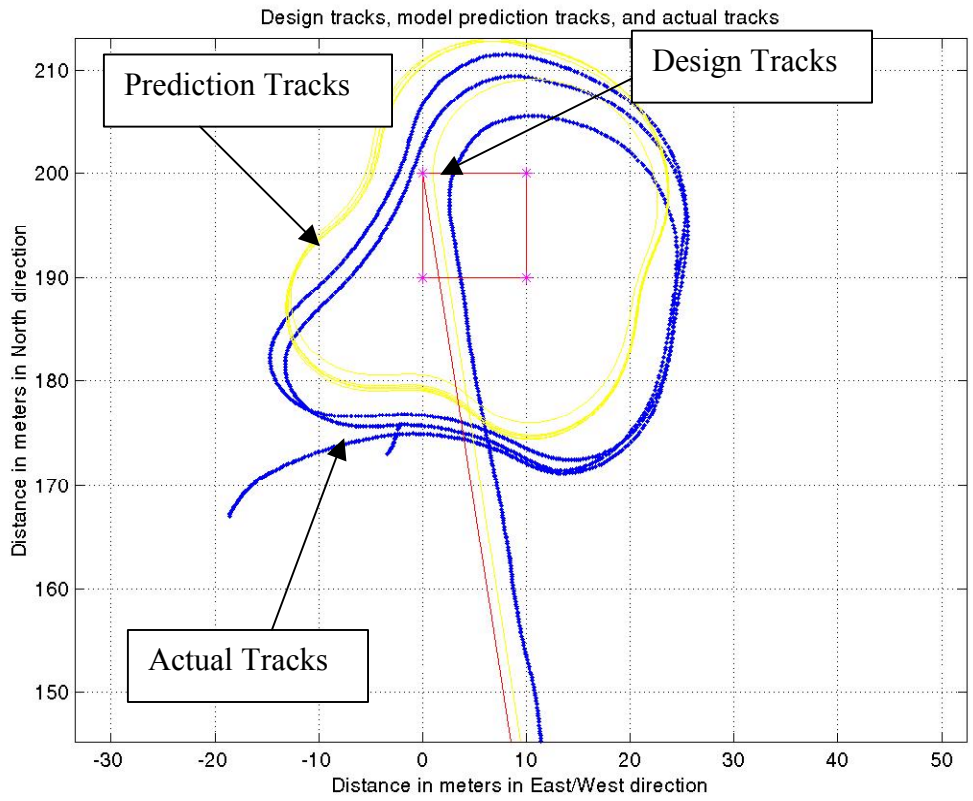

Figure 30. Design Tracks, Model Prediction Track and Actual Tracks with Simulated Southeast Current.

V. CONCLUSIONS

A. SUMMARY

Several factors are of primary concern for Autonomous Underwater Vehicles (AUV) as a viable platform for missions such as minefields, reconnaissance, ocean floor surveys, and decision making in the conduct of amphibious operations in shallow water. These factors include reliability, accuracy, and a high precision navigation system for its submerged operations. Ocean floor data collected for decision making can be meaningful if, and only if, the precise position of the vehicle is known at the time the information is recorded. The challenge of obtaining a highly accurate vehicle position during submerged navigation is ever present. This thesis analyzed the navigation errors during submerged operations of the Autonomous Underwater Vehicle Aries on August 10-12, 2001. Navigation errors were computed as a function of the distance the AUV Aries traveled while submerged. These errors also take into consideration the number of satellites that were available to the AUV Aries during pop-up maneuvers and the figure of merit of the Global Positioning System (GPS). Model prediction tracks with and without current conditions were simulated in MATLAB and compared to the actual tracks. Analysis of the differences between the two tracks provided insight into the cross track error steering, line of sight steering and rudders response time.

B. RESULTS

Navigation errors for the AUV Aries during the Azores operations was found to be anywhere between 2.22% to 2.72% of the distance the Aries traveled while the vehicle was submerged.

- Error is based on the analysis of thirteen pop-up maneuvers and the comparison of the distance differences between the GPS and the vehicles' own internal navigation system. Error was found to be 2.44% of the distance traveled. All data points were scattered around the straight line.
- Error is based on the analysis of eight pop-up maneuvers and comparison of the distance differences between the GPS and the vehicles' own internal navigation system. Five pop-up maneuvers were eliminated because the number of satellites available at the time of the pop-up was less than three. Error was found to be 2.44% of distance traveled.
- Error is based on the analysis of five pop-up maneuvers and the comparison of the distance differences between the GPS and the vehicles'

own internal navigation system. Eight pop-up maneuvers were eliminated because the GPS figure of merit was too high. Error was found to be 2.72 of distance traveled. All data points fitted with the line almost perfectly.

C. RECOMMENDATIONS

To record meaningful data sets, it is necessary to have an accurate vehicle location at the time information is recorded. When continually conducting missions such as minefield, reconnaissance, mine identification, and mine sweeping on enemy shorelines, the AUV must be able to operate independently and covertly to avoid detection by enemies. Unlike the former Soviet Union, our current and future adversary's coastal defenses consist of low technology surface search radar, observation posts and defensive mine warfare. Continuous surfacing by the AUV to receive GPS signals and correct vehicle position could result in enemy detection from their observation posts. The decision making process in the conduct of our amphibious operations in shallow water depends on several factors such as combat air support superiority, Naval gunfire support, and amphibious landing troops and equipment. Our adversaries cannot match the United States in terms of air superiority and Naval gunfire support, but realize that defensive mine warfare is their advantage. Mines carry great destructive power even though they are cheap to produce and do not require sophisticated technology. The current AUV Aries navigation system error of approximately 2.22% of distance traveled while submerged may be unacceptable for long submerged operations. A higher precision navigation gyro compass, costing approximately $75,000 per unit, could reduce errors to 1% of distance traveled.

The vehicle control system should have a means to account for current conditions. Future work should include an investigation of a method for calculating current conditions then continuously feeding them into the feedback control loop. The AUV would then be able to adjust its bow and stern rudders as necessary to compensate for set and drift in order to maintain course and speed. This would be a revolutionary approach for AUV control and navigation systems, which would minimize navigation errors and allow the vehicle to stay submerged longer. The vehicle could avoid continuous surfacing to update the navigation filter with DGPS and enemy detection observation posts. With its continuous feedback loop to adjust the vehicle bow and stern rudders, the AUV could maintain its intended tracks. Our amphibious landing planning team could divide the

enemy's shoreline into sea lanes. The width of the lane would depend on the range of the vehicle camera. The AUV could operate inside its lanes without worrying about current conditions. Information could be recorded and sent back to the mother platform for a decision from our amphibious landing forces.

THIS PAGE INTENTIONALLY LEFT BLANK

APPENDIX A. MATLAB CODE FOR NAVIGATION ERROR VERSUS TIME

```
t=[0 87 169 107 493 546 427 36 37 125 99 327 54 260];
r=[0 2.01 3.56 13.6 20.25 12.16 15.56 1.75 4.35 4.97 6.19 14.12 15.88 13.02];
plot(t,r,'*')
hold
num=sum(t.*r);
den=sum(t.^2);
m=num/den;
P=[m 0];
r1=polyval(P,t);
plot(t,r1)
title('Navigation Filter Error Versus Submerged Time')
xlabel('Time in Seconds')
ylabel('Distance in Meters')
grid
gtext('error=2.44% distance travel')
```

THIS PAGE INTENTIONALLY LEFT BLANK

APPENDIX B. MATLAB CODE FOR NAVIGATION ERROR VERSUS TIME FOR NSV MORE THAN FOUR

```
=[0 87 169 493 546 427 36 37 260];
r=[0 2.01 3.56 20.25 12.16 15.56 1.75 4.35 13.02];
plot(t,r,'*')
hold
num=sum(t.*r);
den=sum(t.^2);
m=num/den;
P=[m 0];
r1=polyval(P,t);
plot(t,r1)
title('Navigation Filter Error Versus Submerged Time For NSv More Than Four')
xlabel('Time in Seconds')
ylabel('Distance in Meters')
grid
gtext('error=2.22% distance travel')
```

THIS PAGE INTENTIONALLY LEFT BLANK

APPENDIX C. MATLAB CODE FOR NAVIGATION ERROR VERSUS TIME HDOP BETWEEN 1.2 - 1.7

```
t=[0 87 169 493 36 260];
r=[0 2.01 3.56 20.25 1.75 13.02];
plot(t,r,'*')
hold
num=sum(t.*r);
den=sum(t.^2);
m=num/den;
P=[m 0];
r1=polyval(P,t);
plot(t,r1)
title('Navigation Filter Error Versus Submerged Time For Hdop Less Than Two')
xlabel('Time in Seconds')
ylabel('Distance in Meters')
grid
gtext('error=2.72% distance travel')
```

THIS PAGE INTENTIONALLY LEFT BLANK

APPENDIX D. MATLAB CODE FOR THE NEW-CTE-BOX PATTERN

```
whitebg('w');
% State = [v r psi]
clear
%load in experrimental data

load d081101_02.d;d=d081101_02;clear d081101_02;
Xd        = d(:,10);
Yd        = d(:,11);
psid      = d(:,16);
drd               = d(:,37);
ud        = d(:,17);
vd        = d(:,18);
rd        = d(:,23);
Second    = d(:,8);




TRUE  = 1;
FALSE = 0;

DegRad = pi/180;
RadDeg = 180/pi;
%State Model PArameters
W   = 600.0;
U = 1.4*3.28;
g = 32.174;
Boy = 500.0;
xg  = 0.125/12.0;
m = W/g;

rho = 1.9903;
L = 10;

Iz = (1/12)*m*(1.33^2 + 10^2); % Approx. Using I = 1/12*m*(a^2 + b^2)

Iz = Iz*5.0;

Yv_dot = -0.03430*(rho/2)*L^3;
Yr_dot = -0.00178*(rho/2)*L^4;
Yv = -0.10700*(rho/2)*L^2;
```

```
Yr = 0.01187*(rho/2)*L^3;
Ydrs = (0.01241*(rho/2)*L^2)/2.0; % Since Bow & Stern Lower Rudders Removed
Ydrb = (0.01241*(rho/2)*L^2)/2.0;

Nv_dot = -0.00178*(rho/2)*L^4;
%Nr_dot = -0.00047*(rho/2)*L^5;
Nr_dot = -Iz;
Nv = -0.00769*(rho/2)*L^3;
Nr = -0.00390*(rho/2)*L^4;
%Ndrs = -2.6496/2.0; % Since Bow & Stern Lower Rudders Removed
%Ndrb = 1.989/2.0;

% Below Modified on 7/12/00 The 3.5 and 3.4167 is the Moment Arm Length in Feet

Ndrs = -0.01241*(rho/2)*(L^2)*(3.5)/2.0; % Since Stern Lower Rudder Removed
Ndrb = 0.01241*(rho/2)*(L^2)*(3.4167)/2.0; % Since Bow Lower Rudder Removed

% Combining Stern & Bow Rudder Effectivness

Ndr = Ndrs - Ndrb;
Ydr = Ydrs - Ydrb; % Cancel Out

m1 = m - Yv_dot;
m2 = m*xg - Yr_dot;
m3 = m*xg - Nv_dot;
m4 = Iz - Nr_dot;

Y1 = Yv;
Y2 = Yr;
Y3 = U^2*Ydr;

N1 = Nv;
N2 = Nr;
N3 = U^2*Ndr;

A = [Y1*U Y2*U;N1*U N2*U];
B = [Y3 N3]';

M = [m1 m2;m3 m4];

A1 = inv(M)*A;
B1 = inv(M)*B;

A = [A1(1,1) A1(1,2) 0;
    A1(2,1) A1(2,2) 0;
     0 1 0];
```

```
B = [B1;0];

dt = 0.125;

t = [0:dt:3000]';

size(t)
% set initial conditions
start=10;
v(1)   = vd(start)*3.28;
r(1)   = rd(start)/180*pi;
rRM(1) = r(1);
psi(1) = psid(start)./180*pi;

% This is the Initial Position of the Vehicle
X(1) = Xd(start); % Meters
Y(1) = Yd(start);

Icte(1) = 0.0;

% Convert to Feet

%X = (2/3)*Y + 3.333333;
%this data from track.out file
No_tracks=24;
Track=[200.0   0.0  2.75 2.75  0  1.25  2.00 0 25.00 8.00 40.00
200.0   10.0  2.75 2.75  0  1.25  2.00 0 25.00 2.00 40.00
190.0   10.0  2.75 2.75  0  1.25  2.00 0 25.00 2.00 40.00
190.0    0.0  2.75 2.75  0  1.25  2.00 0 25.00 2.00 40.00
200.0    0.0  2.75 2.75  0  1.25  2.00 0 25.00 2.00 40.00
200.0   10.0  2.75 2.75  0  1.25  2.00 0 25.00 2.00 40.00
190.0   10.0  2.75 2.75  0  1.25  2.00 0 25.00 2.00 40.00
190.0    0.0  2.75 2.75  0  1.25  2.00 0 25.00 2.00 40.00
200.0    0.0  2.75 2.75  0  1.25  2.00 0 25.00 2.00 40.00
200.0   10.0  2.75 2.75  0  1.25  2.00 0 25.00 2.00 40.00
190.0   10.0  2.75 2.75  0  1.25  2.00 0 25.00 2.00 40.00
190.0    0.0  2.75 2.75  0  1.25  2.00 0 25.00 2.00 40.00
200.0    0.0  2.75 2.75  0  1.25  2.00 0 25.00 2.00 40.00
200.0   10.0  2.75 2.75  0  1.25  2.00 0 25.00 2.00 40.00
190.0   10.0  2.75 2.75  0  1.25  2.00 0 25.00 2.00 40.00
190.0    0.0  2.75 2.75  0  1.25  2.00 0 25.00 2.00 40.00
200.0    0.0  2.75 2.75  0  1.25  2.00 0 25.00 2.00 40.00
200.0   10.0  2.75 2.75  0  1.25  2.00 0 25.00 2.00 40.00
190.0   10.0  2.75 2.75  0  1.25  2.00 0 25.00 2.00 40.00
190.0    0.0  2.75 2.75  0  1.25  2.00 0 25.00 2.00 40.00
```

```
200.0    0.0  2.75 2.75  0  1.25  2.00 0 25.00 2.00 40.00
200.0   10.0  2.75 2.75  0  1.25  2.00 0 25.00 2.00 40.00
190.0   10.0  2.75 2.75  0  1.25  2.00 0 25.00 2.00 40.00
190.0    0.0  2.75 2.75  0  1.25  2.00 0 25.00 2.00 40.00




];
track=Track(:,1:2);




% readin wayopoints from track data assumes track is loaded
for j=1:No_tracks,
   X_Way_c(j)     = track(j,1);
   Y_Way_c(j)     = track(j,2); end;


%Set start position

PrevX_Way_c(1) = Xd(start);
PrevY_Way_c(1) =  Yd(start);

r_com = 0.0;

W_R = 4.0;loiter=0;

a = A1(2,2);
b = B1(2);




a = -.3;
b = (9/24)*a;



x(:,1) = [v(1);r(1);psi(1)];
```

```
% Below are in British Units for CTE Stable Poly
Lam1 = 2.0;
Lam2 = 2.0;
Lam3 = 0.5;
Lam4 = 0.2;

% Below are in British Units for CTE Sliding Mode
%Lam1 = 0.75;
%Lam2 = 0.5;

Lam1 = 2.0;
Lam2 = 1.0;


Eta_FlightHeading = 1.0;
Phi_FlightHeading = 0.5;

% Below for tanh
Eta_CTE = 0.1;
Eta_CTE_Min = 1.0;
Phi_CTE = 0.5;

  Uc = [];
  Vc = []

INT = 0;

PLOT_PART = 0;
SegLen(1) = sqrt((X_Way_c(1)-PrevX_Way_c(1))^2+(Y_Way_c(1)-
PrevY_Way_c(1))^2);
psi_track(1) = atan2(Y_Way_c(1)-PrevY_Way_c(1),X_Way_c(1)-PrevX_Way_c(1));

        for j=2:No_tracks,

                    SegLen(j) = sqrt((X_Way_c(j)-X_Way_c(j-1))^2+(Y_Way_c(j)-
Y_Way_c(j-1))^2);
      psi_track(j) = atan2(Y_Way_c(j)-Y_Way_c(j-1),X_Way_c(j)-X_Way_c(j-1));

   end;
```

```
   SurfPhase =0.0*ones(1,No_tracks);

   j=1;
  Sigma = [];
  Depth_com = [];
  dr=[];
  drl = zeros(1,length(t));

  Depth_com(1) = 5.0;
  WayPointVertDist_com = 5*ones(1,No_tracks);


SURFACE_TIMER_ACTIVE = FALSE;
SurfaceTime = 30.0;

for i=1:length(t)-1,
                    %for i=1:20,

   Depth_com(i) = WayPointVertDist_com(j);

   X_Way_Error(i) = X_Way_c(j) - X(i);
   Y_Way_Error(i) = Y_Way_c(j) - Y(i);

   % DeWrap psi to within +/- 2.0*pi;
   psi_cont(i) = psi(i);

   while(abs(psi_cont(i)) > 2.0*pi)
     psi_cont(i) = psi_cont(i) - sign(psi_cont(i))*2.0*pi;
   end;

   psi_errorCTE(i) = psi_cont(i) - psi_track(j);

   % DeWrap psi_error to within +/- pi;
   while(abs(psi_errorCTE(i)) > pi)
     psi_errorCTE(i) = psi_errorCTE(i) - sign(psi_errorCTE(i))*2.0*pi;
   end;


% **  Always Calculate this
      Beta = v(i)/U;
      Beta = 0.0;
```

```
    cpsi_e = cos(psi_errorCTE(i)+Beta);
    spsi_e = sin(psi_errorCTE(i)+Beta);


    s(i) = [X_Way_Error(i),Y_Way_Error(i)]*...
          [(X_Way_c(j)-PrevX_Way_c(j)),(Y_Way_c(j)-PrevY_Way_c(j))]';
    % s is distance to go projected to track line(goes from 0-100%L)

    s(i) = s(i)/SegLen(j);

    Ratio=(1.0-s(i)/SegLen(j))*100.0;
% **

    % radial distance to go to next WP
    ss(i) = sqrt(X_Way_Error(i)^2 + Y_Way_Error(i)^2);

    % dp is angle between line of sight and current track line
    dp(i) = ...
          atan2( (Y_Way_c(j)-PrevY_Way_c(j)),(X_Way_c(j)-PrevX_Way_c(j)) )...
        - atan2( Y_Way_Error(i),X_Way_Error(i) );

    if(dp(i) > pi),
      dp(i) = dp(i) - 2.0*pi;
    end;

    cte(i) = s(i)*sin(dp(i));


    if( abs(psi_errorCTE(i)) >= 40.0*pi/180.0) | (s(i) < 0.0 |((loiter==1)& s(i)<20) )
     % Use LOS Control
     LOS(i)=1;
     psi_comLOS = atan2(Y_Way_Error(i),X_Way_Error(i));

      psi_errorLOS(i) = psi_comLOS - psi_cont(i);

      if(abs(psi_errorLOS(i)) > pi),
        psi_errorLOS(i) = ...
        psi_errorLOS(i) - 2.0*pi*psi_errorLOS(i)/abs(psi_errorLOS(i));
      end;

      Sigma_FlightHeading = 0.9499*(r_com - r(i)) + 0.1701*psi_errorLOS(i);

      dr(i) = -1.5435*( 2.5394*r(i) ...
            + Eta_FlightHeading*tanh(Sigma_FlightHeading/Phi_FlightHeading));

  else
```

```
    % Use CTE Controller
LOS(i)=0;                       if(cpsi_e ~= 0.0), % Trap Div. by Zero !

%    STABLE POLY Soln

%       dr(i) =   (1.0/(U*b*cpsi_e))*(-U*a*r(i)*cpsi_e + U*r(i)^2*spsi_e ...
%             - Lam1*U*r(i)*cpsi_e - Lam2*U*spsi_e - 3.28*Lam3*cte(i) ...
%             - Lam4*Icte);

%      dr(i) =   (1.0/(U*b*cpsi_e))*(-U*a*rRM(i)*cpsi_e + U*rRM(i)^2*spsi_e ...
%            - Lam1*U*rRM(i)*cpsi_e - Lam2*U*spsi_e - 3.28*Lam3*cte(i) ...
%            - Lam4*Icte);

%    SMC Soln

%      Eta_CTE = Eta_CTE_Min + 0.5*abs(cte(i));

     Sigma(i) = U*rRM(i)*cpsi_e + Lam1*U*spsi_e + 3.28*Lam2*cte(i);

     dr(i) =   (1.0/(U*b*cpsi_e))*(-U*a*rRM(i)*cpsi_e + U*rRM(i)^2*spsi_e ...
   - Lam1*U*rRM(i)*cpsi_e - Lam2*U*spsi_e - Eta_CTE*(Sigma(i)/Phi_CTE));

%      dr(i) =   (1.0/(U*b*cpsi_e))*(-U*a*rRM(i)*cpsi_e + U*rRM(i)^2*spsi_e ...
%      - Lam1*U*rRM(i)*cpsi_e - Lam2*U*spsi_e) ...
%      - Eta_CTE/sign(U*b*cpsi_e)*Sigma(i)/Phi_CTE;
%      - Eta_CTE/sign(U*b*cpsi_e)*tanh(Sigma(i)/Phi_CTE);

                                    else

                                dr(i) = dr(i-1);

                                    end;
    % Int of CTE in meters-sec
                        if(INT==1),
      Icte = Icte + dt*cte(i);
                        else
      Icte = 0.0;
                        end;

    UseVector(i,:) = [1 t(i)];

                                     end; % End of CTE Controller

  % use LOS if near to loiter point
```

```
                %       if (loiter==1)& s(i)<10;  dr(i)=drlos(i);end;

% Surface Phase Logic (Independent of LOS or CTE)

   if(SurfPhase(j) == TRUE)
     if(SURFACE_TIMER_ACTIVE == FALSE)
       if(Ratio > 40.0)
         % Start a Timer
         SURFACE_TIMER_ACTIVE = TRUE;
         Depth_com(i) = 0.0;
         SurfaceWait = SurfaceTime + t(i);
         SurfaceWait
       end;
     end;
   end;

   if(SURFACE_TIMER_ACTIVE == TRUE)
    if(t(i) >= SurfaceWait)
      SURFACE_TIMER_ACTIVE = FALSE;
      Depth_com(i) = WayPointVertDist_com(j);
      SurfPhase(j) = 0;
    else
      Depth_com(i) = 0.0;
    end;
   end;

%if(i==800)
%    X(1,i) = 20.0;
% end;

 %if(i==2500)
 %   X(1,i) = 60.0;
 %end;



                if(abs(dr(i)) > 0.4)
                        dr(i) = 0.4*sign(dr(i));
                end;



%dr(i) = 22.5*pi/180;


% Model drl is the actual lagged rudder, dr is the rudder command.
```

```
 taudr=0.255;

 drl(i+1)=drl(i)+dt*(dr(i)-drl(i))/taudr;
 %     if(abs(drl(i)) > 0.4)
 %                          drl(i) = 0.4*sign(drl(i));
%                end;


 %Jay Johnson Model;
 Yv = -68.16;
 Yr = 406.3;
 Ydr = 70.0;
 Nv = -10.89;
 Nr = -88.34;
 Ndr = -35.47;

 MY = 456.76;
 IN = 215;

 M=diag([MY,IN,1]);
 AA=[Yv,Yr,0;Nv,Nr,0;0,1,0];BB=[Ydr;Ndr;0];
 A=inv(M)*AA;B=inv(M)*BB;

  x_dot(:,i+1) = [ A(1,1)*v(i) + A(1,2)*r(i) + B(1)*drl(i);
              A(2,1)*v(i) + A(2,2)*r(i) + B(2)*drl(i);
              r(i)];

   x(:,i+1)=x(:,i)+dt*x_dot(:,i);
  v(i+1)   = x(1,i+1)/12;
  r(i+1)   = x(2,i+1);
  psi(i+1) = x(3,i+1);
  rRM(i+1)=r(i+1);

%  Throw in some Waves
  %Uc(i) = -0.5*sin(2*pi*t(i)/5);
  %Vc(i) =  0.5*sin(2*pi*t(i)/5);

  %Model using system ID results from Bay tests

 %  rRM(i+1) = rRM(i) + dt*(a*rRM(i) + b*drl(i));
 %  psi(i+1) = psi(i) + dt*rRM(i);
  % side slip added proprtional to turn rate from AZORES data V in ft/sec
 % v(i+1) = 1.0*rRM(i+1)*3.28;

   Uc = -0.15;%*0.0;Northernly current
   Vc = 0.15;%*0.0;Westerly Current
```

```
  %Kinematics
  X(i+1) = X(i) + (Uc + (U/3.28)*cos(psi(i)) - v(i)/3.28*sin(psi(i)) )*dt;
  Y(i+1) = Y(i) + (Vc + (U/3.28)*sin(psi(i)) + v(i)/3.28*cos(psi(i)) )*dt;

  %  Check to See if we are Within the Watch_Radius


  if(sqrt(X_Way_Error(i)^2.0 + Y_Way_Error(i)^2.0) <= W_R | s(i) < 0.0),

    if (loiter~=1); %insert this for loiter node
      INT = 1;
      if(j==No_tracks),
      PLOT_PART = 1;
                          break;
        end;
    PrevX_Way_c(j+1) = X_Way_c(j);
    PrevY_Way_c(j+1) = Y_Way_c(j);
    j=j+1;
        end;
  end;

end;

%end update loop
%update
dr(i+1) = dr(i);
cte(i+1) = cte(i);
s(i+1) = s(i);
ss(i+1) = ss(i);

if(PLOT_PART),

  figure(1);clf,
  plot(t([1:i+1]),psi*180/pi,t([1:length(psid)]),psid,'g.');
  hold;
  plot(t([1:i+1]),dr*180/pi,'r',t([1:length(psid)]),drd,'g.');grid;
  TITLE('psi in basic color, dr in red');
  hold;zoom on;

  figure(2);clf,

  plot(t([1:i+1]),cte,'b',t(1:length(LOS)),LOS,'y');
  hold;

  plot(t([1:length(s)]),s,'r');TITLE('cte in blue,LOS in yellow, s in red')
```

```
   hold;zoom on;grid


else

   figure(1);clf,
   plot(t,psi*180/pi);
   hold;
   plot(t,drl*180/pi,'r');
   hold;grid;
   figure(2);
   plot(t,cte,'b',t(1:length(LOS)),LOS,'y');
   hold;
   plot(t,s,'r');
   plot(t,ss,'g');grid;
   TITLE('s in red,ssin green, cte in blue')
   hold;zoom on;

end;


   figure(3);clf,
   plot(Yd,Xd,'b.',Y,X,'y');grid;
   hold
   plot([Y_Way_c(1) PrevY_Way_c(1)],[X_Way_c(1) PrevX_Way_c(1)],'r');
   plot(Y_Way_c,X_Way_c,'r');
   plot(Y_Way_c,X_Way_c,'m*'),
   hold;zoom on;

   figure(4), clf,
   plot(t([1:i+1]),r*180/pi,'r',t([1:length(psid)]),rd,'g.');grid;

   figure(5),clf,plot(t([1:i+1]),vd(1:i+1),'r',t([1:i+1]),v,'g.')
```

LIST OF REFERENCES

1. Healey, A. J. Marco, D. B., "Command, Control and Navigation: Experimental Results with the NPS ARIES AUV" IEEE Journal of Oceanic Engineering, October 2001. Vol. 26, No. 4, pp. 466-476.

2. Healey, A. J., Marco, D. B., "Current Developments in Underwater Vehicle Control and Navigation: The NPS ARIES AUV", Proceedings of IEEE Oceans 2000, Providence, RI, September 2000.

3. Marco, D. B., "Phoenix AUV for Mine Reconnaissance/Neutralization in Very Shallow Waters," Component Configuration Drawing for AUV Fest 98, December 1998.

4. Healey, A. J. and Brutzman, D. P., "Autonomous Underwater Vehicle Technology" The Ocean Engineering Society of the IEEE, June 1996.

5. Healey, A. J. and Marco, D. B., "On Line Compensation of Heading Sensor Bias for Low Cost AUVs" Proceeding IEEE, August 1998.

6. Bachmann, E. R., Healey, A. J., Knapp, R. G., McGhee, R. B., Roberts, R. L., Whalen, R. H., Yun, X. and Zyda, M. J., "Testing and Evaluation of an Integrated GPS/INS System for Small AUV Navigation" IEEE Journal of Oceanic Engineering, Vol. 24, No. 3, July 1999.

7. Healey, A. J. and Lienard, D., "Multivariable Sliding Mode Control for Autonomous Diving and Steering of Unmanned Underwater Vehicles" IEEE Journal of Oceanic Engineering, Vol. 114, No. 3, July 1993.

8. Healey, A. J., Park, J. and Smith S. M., "Asynchronous Data Fusion for AUV Navigation Via Heuristic Fuzzy Filtering Techniques" Proceeding IEEE, October 1997.

9. Kanayama, Y. and Hartman, B. I., "Smooth Local Path Planning for Autonomous Vehicles" Autonomous Robot Vehicles, Springer-Verlag, ISBN 000-387-97240, pp. 62-68, 1990.

10. McGhee, Y. and Healey, A. J., "An Integrated GPS/INS Navigation System for Small AUV's Using an Asynchronous Kalman Filter", Proceeding IEEE, August 1998.

THIS PAGE INTENTIONALLY LEFT BLANK

INITIAL DISTRIBUTION LIST

1. Defense Technical Information Center
   Ft. Belvoir, Virginia

2. Dudley Knox Library
   Naval Postgraduate School
   Monterey, California

3. Mechanical Engineering Department
   Chairman, Code ME
   Naval Postgraduate School
   Monterey, California

4. Professor Anthony J. Healey, Code ME
   Naval Postgraduate School
   Monterey, California

5. Dr. T. B. Curtin, Code 3220M
   Office of Naval Research
   Arlington, Virginia

6. Dr. Douglas Todoroff, Code 321
   Office of Naval Research
   Arlington, Virginia

7. Dr. Tom Sweane, Code 3210E
   Office of Naval Research
   Arlington, Virginia

8. Dr. Antonio Pascal
   Institute of Systems and Robotics
   Instituto Superior Technico
   Codex, Portugal

9. Mr. Larry Grace
   San Jose, California

10. LCDR Thanh V. Nguyen
    Supervisor of Shipbuilding
    Mayport, Florida